Journal of Genetic Engineering and Biotechnology 23 (2025) 100495

Contents lists available at ScienceDirect

Journal of Genetic Engineering and Biotechnology

journal homepage: www.elsevier.com/locate/jgeb

Assessment of the gold nanoparticles biosynthesized using *Casuarina equisetifolia* bark extract against the ethion induced Hepato- and neurotoxicity in rats

Wael Mahmoud Aboulthana [a,*], Noha El-Sayed Ibrahim [b], Amal Gouda Hussien [a], Amgad Kamal Hassan [a], Wagdy K.B. Khalil [c], Hassan Abdel-Gawad [d], Hamdy Ahmed Taha [d], Ayda K. Kelany [e], Kawkab A. Ahmed [f]

[a] *Biochemistry Department, Biotechnology Research Institute, National Research Centre, 33 El Bohouth St., P.O. 12622, Dokki, Giza, Egypt*
[b] *Microbial Biotechnology Department, Biotechnology Research Institute, National Research Centre, 33 El Bohouth St., P.O. 12622, Dokki, Giza, Egypt*
[c] *Cell Biology Department, Biotechnology Research Institute, National Research Centre, 33 El Bohouth St., P.O. 12622, Dokki, Giza, Egypt*
[d] *Applied Organic Chemistry Department, Chemical Industries Researches Institute, National Research Centre, 33 El Bohouth St., P.O. 12622, Dokki, Giza, Egypt*
[e] *Department of Genomic Medicine, Cairo University Hospitals, Cairo University, Giza, Cairo, Egypt*
[f] *Department of Pathology, Faculty of Veterinary Medicine, Cairo University, Giza 12211, Egypt*

A R T I C L E I N F O

Keywords:
Ethion
Casuarina equisetifolia Bark
Gold Nanoparticles
Electrophoresis
Isoenzymes
Gene Expression

A B S T R A C T

Ethion (Etn) is classified as an organophosphate pesticide (OP) that causes toxicity even at low concentrations and targets the liver, brain, kidney, and blood. Gold nanoparticles (Au-NPs) were biosynthesized from the whole methanolic extract of *Casuarina equisetifolia* bark, and their efficacy against Etn-induced hepato- and neurotoxicity in rats was assessed. In addition to determining conventional biochemical measurements, the target tissues (liver and brain) were examined for oxidative stress, inflammatory, and fibrotic markers. The protein and isoenzyme patterns were also assayed using an electrophoretic technique. Additionally, apoptotic gene expression was measured. The target tissues were also subjected to histopathological analysis. In all groups treated with *C. equisetifolia* bark gold nano-extract, it was observed that the levels of the hematological measurements that were impacted by the oral injection of Etn had recovered to normal. Regarding the biochemical measurements, the group that received nano-extract pretreatment showed greater improvement than the therapeutic group. The levels of inflammatory indicators significantly decreased ($p \leq 0.05$), while the antioxidant system markers increased in both liver and brain tissues in the group that received the nano-extract beforehand. In both target tissues, especially in the pre-treated group, the nano-extract reduced the severity of the Etn-caused lesions. During electrophoretic assays, the nano-extract in the pre-treated group prevented the qualitative alterations indicated by the lowest similarity index (SI%) values of the Etn-injected group compared to the normal group. The molecular assay showed that the nano-extract reduced the expression of apoptotic genes that were markedly elevated in the Etn-injected rats, but it was unable to return their values to normalcy. The study concluded that in the group that received nano-extract pretreatment, the biochemical, histopathological, physiological, and molecular abnormalities caused by Etn were reduced by the *C. equisetifolia* bark gold nano-extract.

1. Introduction

Organophosphate pesticides (OPs) are chemical agents used widely in agriculture, households, and veterinary settings.[1] They affect the nervous system, which is their primary target, by over-stimulating the cholinergic pathways due to a lack of activity of butyrylcholinesterase (BChE) and acetylcholinesterase (AChE) enzymes.[2] Both acute and chronic doses of these substances cause neurotoxicity and target the brain.[3] By blocking AChE, which hydrolyzes acetylcholine (a neurotransmitter) in cholinergic synapses in the central and peripheral nervous systems, high concentrations of these chemical toxicants can cause negative side effects such as headache, confusion, convulsions, coma, muscle paralysis resulting in respiratory failure, and death.[4] .

The development of neurodegenerative diseases has been linked to

* Corresponding author.
E-mail addresses: wmkamel83@hotmail.com, wm.kamel@nrc.sci.eg (W.M. Aboulthana).

https://doi.org/10.1016/j.jgeb.2025.100495
Received 12 March 2025; Received in revised form 7 April 2025; Accepted 11 April 2025

them. Oxidative and nitrosative stress, disruption of mitochondrial bioenergetics, and disturbance of mitochondrial dynamics are the most common ways that OPs produce neurotoxicity.[5] These toxicants have detrimental consequences that include reactive gliosis and an increase in glial fibrillary acidic protein, which ultimately result in neuronal degeneration in the cortex and hippocampus.[6] OPs like Ethion (Etn) (O, O,O,O-tetraethyl S,S-methylene bis-(phosphorodithioate)) are still used extensively in Egypt and have had an impact on public health.[7] Even at modest doses, it has an impact on laboratory animals' liver, kidney, brain, and blood.[8] It reduces the antioxidant defense in the brain and erythrocytes by changing the endogenous (enzymatic and non-enzymatic) antioxidants.[9] Furthermore, in addition to DNA damage, mitochondrial dysfunction, and therefore apoptosis, it may cause hepatocellular injury and damage to the liver tissue.[10–11] .

It is possible for metal nanoparticles (M−NPs) that are smaller than cellular organelles (less than 100 nm) to move through biological structures and circulate inside the circulatory system.[12–13] They can also interact with biological systems, including cells and tissues.[14] Because of their unique physicochemical properties, M−NPs can be used to novel therapeutic and diagnostic approaches. These features include the presence of targeting moieties on the particle surface, size, hydrophilicity, and surface charge.[15–16] They increase the therapeutic effectiveness of traditional drugs by improving their solubility and biodistribution. This is because they can overcome obstacles that usually limit the efficacy of commercially available macro- and micromolecular drugs.[17] The gold nanoparticles (Au-NPs) are widely used in the biomedical sectors as well as in common items like toothpaste and cosmetics because they are readily surface-functionalized, biocompatible, and produced.[18] It has been demonstrated that Au-NPs are a safe treatment for several autoimmune and inflammatory disorders due to the inert properties of bulk gold.[19–20] Additionally, they show protective benefits against anomalies caused by the overproduction of reactive oxygen species (ROS).[21–22] In comparison to the chemical technique, the biosynthesized M−NPs are energy-efficient, inexpensive, and ecologically benign.[23] In the plant extract, tannins, saponins, flavonoids, amino acids, and carbohydrates make up the bulk of the phytochemicals. These substances can be used as stabilizing and reducing agents during the biosynthesis of M−NPs by utilizing green nanotechnology.[24–25] .

The "*Casuarinaceae*" family includes *Casuarina equisetifolia*.[26] It is rich in a variety of physiologically active secondary metabolites, including gallic acid, ellagic acid, quercetin, catechin, d-gallocatechin, and coumaroyl triterpenes, which have cytotoxic and antioxidant qualities. It is also known to store tannin. It can thus be used to treat a wide range of ailments, such as fever, diarrhea, dysentery, headache, cough, ulcers, and toothaches.[27–28] Au-NPs biosynthesised utilizing bark extract from *C. equisetifolia* shown a hepato- and neuroprotective benefit against the abnormalities caused by chlorpyrifos, according to **Aboulthana *et al.*.**[29] Thus, the primary objective of the present work was to investigate the protective and therapeutic effects of *C. equisetifolia* bark gold nano-extract against Eth toxicity in rats.

2. Materials and Methods

2.1. Synthesis of gold nanoparticles using the extract

According to **Aboulthana *et al.*,**[30] Au-NPs were biosynthesized using the methanolic extract of *C. equisetifolia* bark. A nanoemulsion was prepared using crude plant extracts, the non-ionic surfactant Tween 20 (HLB-16.7), cellulose nanocrystals (CNC), and water via the spontaneous emulsification method. The process was carried out in two steps. In the first step, the organic phase was created by mixing the plant crude sample with the chosen surfactant (Tween 20) at a ratio of 1:5, then 3 gm of CNC was added, and the mixture was sonicated for 30 min. In the second step, the organic phase (plant extract, Tween 20, and CNC) was added drop by drop (20 mL/min) to water using a separating funnel and stirring the system magnetically at 800 rpm (60 °C) for 5 h. Subsequently, the prepared Au-NPs were added to the prepared nanoemulsion at a ratio of 1 %. The mixture was sonicated at 50 °C for another 30 min.

2.2. Administration of gold C. Equisetifolia nano-extract

The nano-extract's median lethal dose (LD_{50}) was around 9333.33 mg/kg as proposed by **Aboulthana *et al.*.**[30] and presented in Supplementary Table 1. Therefore, in the *in vivo* study, the ideal dose for oral administration is considered to be 1/10 of LD_{50}, and it was found to be 933.33 mg/kg b.w.

2.3. Induction of toxicity

Rats were orally given the Etn solution in dimethyl sulfoxide (DMSO) at a dose of 20.8 mg/kg b.w. based on the study demonstrated by **Raj *et al.*.**[31] .

2.4. Experimental design

Fifty (50) mature male Wistar rats (weighing 120——150 gm) were housed in the Animal House at the National Research Center in Giza, Egypt. Each cage contained ten rats.

The control group was orally administered DMSO for 28 days. The gold nano-extract treated group was administered gold nano-extract for 21 days. The Etn- intoxicated group was given Etn as a single dose daily for 28 days. The gold nano-extract pre-treated (protected) group was given Etn for 28 days after 21 days of receiving gold nano-extract. The

Table 1
Effect of the *C. equisetifolia* gold nano-extract against the changes induced by ethion (Etn) in markers of the antioxidant system in both liver and brain tissues of rats.

		C.	*C. equisetifolia* gold nano-extract	Etn	Etn + *C. equisetifolia* gold nano-extract	
					Pre-treated	Post-treated
Liver	**TAC** (μmol/g)	37.77 ± 0.04	37.75 ± 0.07	13.37 ± 0.02[a]	38.29 ± 0.04[b]	24.28 ± 0.05[ab]
	GSH (mg/g tissue)	18.71 ± 0.05	18.64 ± 0.02	6.62 ± 0.02[a]	18.97 ± 0.05[b]	12.03 ± 0.02[ab]
	SOD (IU/g tissue)	20.68 ± 0.02	20.69 ± 0.01	7.32 ± 0.01[a]	20.97 ± 0.02[b]	13.29 ± 0.02[ab]
	CAT (IU/g tissue)	12.04 ± 0.06	12.03 ± 0.07	4.26 ± 0.02[a]	12.21 ± 0.07[b]	7.74 ± 0.03[ab]
	GPx (IU/g tissue)	12.07 ± 0.07	12.03 ± 0.06	4.27 ± 0.02[a]	12.23 ± 0.08[b]	7.76 ± 0.04[ab]
Brain	**TAC** (μmol/g)	37.18 ± 0.11	37.20 ± 0.12	13.16 ± 0.04[a]	34.32 ± 0.13[ab]	23.90 ± 0.06[ab]
	GSH (mg/g tissue)	10.64 ± 0.04	10.69 ± 0.01	3.77 ± 0.02[a]	9.82 ± 0.04[ab]	6.84 ± 0.03[ab]
	SOD (IU/g tissue)	15.70 ± 0.02	15.71 ± 0.01	5.56 ± 0.01[a]	14.49 ± 0.03[ab]	10.09 ± 0.02[ab]
	CAT (IU/g tissue)	8.05 ± 0.06	7.99 ± 0.06	2.85 ± 0.02[a]	7.43 ± 0.05[ab]	5.18 ± 0.04[ab]
	GPx (IU/g tissue)	7.10 ± 0.01	7.11 ± 0.01	2.52 ± 0.00[a]	6.56 ± 0.01[ab]	4.57 ± 0.01[ab]

Data were presented as mean ± SE (from five replicates). **a**: Indicates significance at $p \leq 0.05$ compared to the control and **b**: to Etn injected group.

gold nano-extract post-treated (therapeutic) group underwent a 21 day treatment with gold nano-extract after receiving Etn for 28 days.

2.5. Collection of blood samples and tissues

After an 18-hour fast, the final dose of therapy was administered. Following anesthesia, the animals were euthanized by cervical dislocation. Blood samples were collected from the *retro*-orbital plexus for assessing the activity of the AChE enzyme and conducting hematological tests. After allowing the blood samples to coagulate, they were centrifuged for 15 min at 3000 rpm. The separated sera were kept at −20 °C until they were ready for biochemical tests. Following cervical dislocation, the animals' liver and brain tissues were extracted and cleaned in ice-cold saline. For histological analysis, a small number of autopsied sections of these tissues were stored in a 10 % neutral buffered formalin solution. After homogenizing the remaining tissues in potassium phosphate buffer (pH 7.4), they were centrifuged for ten minutes at 3000 rpm. For use in biochemical tests, the clear supernatants were kept in storage at −80 °C. The final portion of the tissues was quickly frozen using liquid nitrogen for molecular analysis.

2.6. Body and organ weights assays

During the trial, body weights were measured three times: at 0, 15, and 30 days. The body weight growth was calculated using the method presented by **Al-Attar**.[32] The relative weight of each rat's body was calculated using the method provided by **Al-Attar and Al-Rethe**[33] after determining the absolute weights of the liver and brain.

2.7. Hematological and biochemical assays

An automated blood analyzer was used to quantify the hematological parameters in heparinized blood samples. In RBC and plasma samples, the acetylcholinesterase (AChE) enzyme activity was assessed using the method developed by **Gorun *et al.***[34] after being proposed by **Ellman *et al.***.[35] The commercially available kits were used to determine the lipid profile and all other standard biochemical parameters in the blood sample, including liver, heart, and kidney functions colorimetrically based on the reaction of the kit chromogen with its specific analyte using a spectrophotometric technique.

2.8. Biochemical assays in tissues homogenates

Clear supernatants of tissue homogenates (liver and brain) were used to measure oxidative stress markers, such as reduced glutathione (GSH),[37] total antioxidant capacity (TAC),[36] and the activity of the enzymes glutathione peroxidase (GPx),[40] catalase (CAT),[39] and superoxide dismutase (SOD).[38] Additionally, the levels of total protein carbonyl (TPC)[42] and lipid peroxidation products (LPO)[41] were measured. Furthermore, two frequent inflammatory indicators, interleukin-6 (IL-6)[43] and tumor necrosis factor-α (TNF-α),[44] were identified using the quantitative sandwich enzyme immunoassay (ELISA). Only the amount of fibrotic markers (hydroxyproline)[45] was measured in liver tissue homogenates. Using a commercially available ELISA kit, the amount of β-amyloid (Aβ) in brain tissue homogenates was measured.[46] .

2.9. Histopathological examination

For this examination, paraffin sections from the preserved specimens (liver and brain) with a thickness of 5 μm were stained using Hematoxylin and Eosin (H&E).[47] The histopathological abnormalities in the liver tissue and the neuropathologic lesions were assessed and scored from five microscopically examined fields per rat in accordance with the following order of procedure proposed by **Fouad and Ahmed**[48]: no changes, mild, moderate, and severe changes (0, 1, 2, and 3, respectively).

2.10. Electrophoretic assays

2.10.1. Native electrophoretic patterns

Known weights (0.2 g) of the tissue (liver and brain) were homogenized in extraction buffer (1 ml). Following homogenization process, the tissue homogenates were centrifuged. To ensure uniform protein concentrations in each well, the Bradford method[49] was used to measure the protein concentration in the supernatants. The protein concentration was then diluted with sample loading dye in proportion to the protein concentration. The protein bands, lipid, and calcium moieties of native proteins were assayed using Coomassie Brilliant Blue (CBB),[50] Sudan Black B (SBB),[51] and Alizarin Red "S"[52] in the vertical slab polyacrylamide gel electrophoresis.

To identify types of the catalase (CAT) and peroxidase (POX) enzymes electrophoretically, the native gel was treated with the particular conditioning buffer and hydrogen peroxide (H_2O_2) as a substrate. It was then stained with potassium iodide (KI)[53] and benzidine.[54] After the native gel was incubated in a soluble starch solution as a substrate, it was stained with iodine solution to identify types of the α-amylase (α-Amy) enzyme.[55] Types of the α- and β-esterase (EST) enzymes were detected by incubating the gel in a reaction mixture containing Fast Blue RR and substrates of α- and β-naphthyl acetate, respectively.[56] .

2.10.2. Data analysis

The colored bands were assessed using Quantity One (Version 4.6.2). The percentages of similarity indices (SI%) between each treatment group and the control were determined using the formula proposed by **Nei and Li**.[57] .

2.11. Molecular assay

The relative expressions of the genes for caspase-3, tumor suppressor (p^{53}), B-cell leukemia/lymphoma (Bcl2), and Bcl2-associated X protein (BAX) were assessed. To isolate total RNA, the tissue samples were homogenized in TRIzol® Reagent (Invitrogen, USA). To verify the integrity of the extracted RNA, formaldehyde-containing agarose gel electrophoresis was used to examine the 28S and 18S bands. The entire RNA was resuspended in water treated with DEPC after any remaining DNA had been digested using RQ1 RNase-free DNase (1U). The extracted Poly (A) + RNA was converted to cDNA using the RevertAid^{TM} First Strand cDNA Synthesis Kit (MBI Fermentas, Germany). The number of copies was calculated usingthe StepOneTM Real-Time PCR System based on the reaction protocol presented by **Aboulthana *et al.***.[29] Melting curve analysis, which was used to evaluate the quality of the specific primers listed in Supplementary Table 2, showed that the melting temperature at the end of each *qPCR* run was 95.0 °C. To determine the relative expression of the targeted genes, each experiment was carried out three times for each target gene using the $2^{-\Delta\Delta CT}$ method.[58] .

2.12. Statistical analysis

A one-way analysis of variance (one-way ANOVA) test was used to analyze the data, which is presented as mean ± standard error (SE) in the tables and figures. A statistically significant difference between the groups is indicated by a "*p*" value of ≤ 0.05.

3. Results

Following the injection of Etn, a number of adverse hematological and biochemical consequences were observed.

3.1. Body and organ weights assays

Throughout the investigation, the body weight gain in the Etn-injected group significantly ($p \leq 0.05$) decreased, as shown in Supplementary Fig. 1**a**. In comparison to the Etn-injected group, the gold nano-

Table 2
Effect of the *C. equisetifolia* gold nano-extract against the alterations in markers of inflammatory and fibrotic reactions induced by ethion (Etn) in both liver and brain tissues of rats.

		C.	*C. equisetifolia* gold nano-extract	Etn	Etn + *C. equisetifolia* gold nano-extract	
					Pre-treated	Post-treated
Liver	**TNF-α** (Pg/g tissue)	344.00 ± 0.95	343.20 ± 0.58	514.00 ± 0.95[a]	395.20 ± 0.66[ab]	416.40 ± 1.60[ab]
	IL-6 (Pg/g tissue)	415.40 ± 1.29	415.60 ± 1.50	620.69 ± 1.61[a]	477.23 ± 1.70[ab]	502.83 ± 2.43[ab]
	Hydroxyproline (μg/mg tissue)	0.32 ± 0.00	0.33 ± 0.01	0.32 ± 0.00	0.32 ± 0.00	0.32 ± 0.00
	AChE (ng/g tissue)	0.55 ± 0.02	0.49 ± 0.03	0.31 ± 0.01[a]	0.45 ± 0.02[b]	0.47 ± 0.02[b]
Brain	**TNF-α** (Pg/g tissue)	133.00 ± 0.55	134.00 ± 0.63	198.4 ± 1.34[a]	152.81 ± 1.03[ab]	161.01 ± 1.36[ab]
	IL-6 (Pg/g tissue)	224.80 ± 1.32	225.60 ± 0.60	335.90 ± 1.96[a]	258.26 ± 1.67[ab]	272.12 ± 2.12[ab]
	β-amyloid (Pg/g tissue)	6.19 ± 0.01	6.19 ± 0.01	9.25 ± 0.03[a]	7.11 ± 0.03[ab]	7.50 ± 0.04[ab]
	AChE (ng/g tissue)	11.21 ± 0.69	11.43 ± 0.50	7.81 ± 0.33[a]	10.07 ± 0.76[b]	10.49 ± 0.70[b]

Data were presented as mean ± SE (from five replicates). **a**: Indicates significance at $p \leq 0.05$ compared to the control and **b**: to Etn injected group.

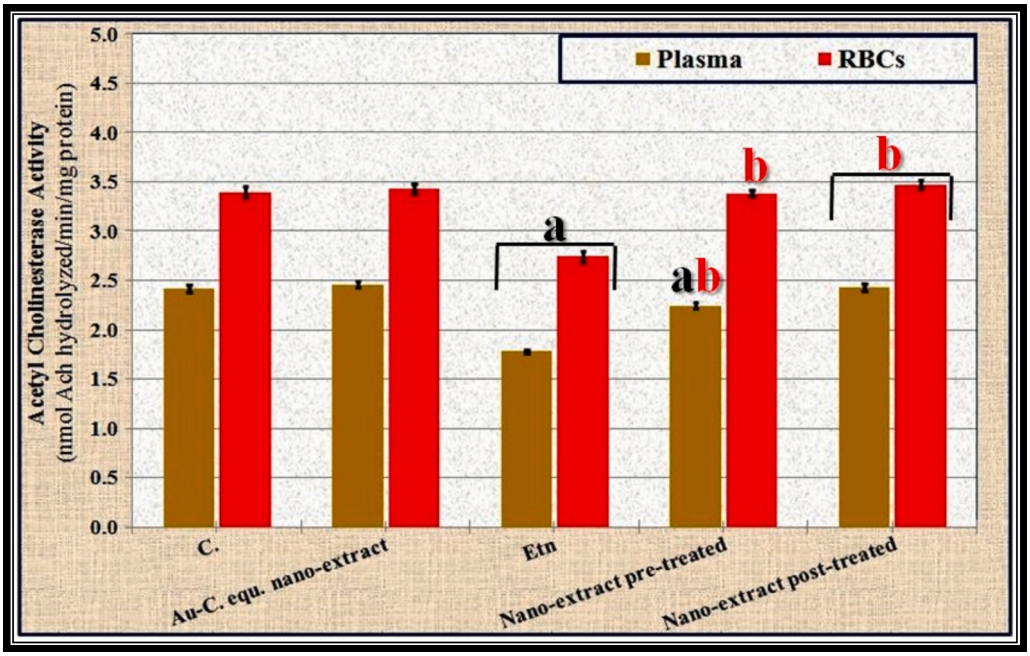

Fig. 1. Effect of the *C. equisetifolia* gold nano-extract against the changes in activity of acetylcholinesterase (AChE) enzyme induced by ethion (Etn) in blood of rats. Data were presented as mean ± SE (from five replicates). **a**: Indicates significance at $p \leq 0.05$ compared to the control and **b**: to Etn injected group.

extract significantly ($p \leq 0.05$) increased body weight gain when given in combination with Etn injection. It significantly ($p \leq 0.05$) decreased body weight when taken alone. It was unable to return body weight to normal levels. Rats treated with Etn had significantly ($p \leq 0.05$) higher absolute and relative organ weights for the liver and brain than the control group (**Supplementary** Fig. 1**b**). Following the administration of the nano-extract, the relative organ weights of the rats decreased compared to those intoxicated with Etn, and by the end of the experiment, their values had returned to normal.

3.2. Hematological measurements

Hematological measurements are regarded as the first sign of toxicity caused by OPs. When compared to the control rats, Etn intoxication significantly ($p \leq 0.05$) lowered the levels of hematological parameters (Supplementary Table 3). Following treatment with nano-extract, these values significantly ($p \leq 0.05$) rose and reverted to normal levels.

3.3. Biochemical measurements

The Etn-injection increased levels of several biomarkers, including liver enzymes, kidney function indicators, cardiac enzymes, and lipid profile significantly ($p \leq 0.05$) compared to the normal rats (Supplementary Table 4). Total protein and albumin levels decreased following the Etn injection, as indicated by the protein assays. The altered biochemical measures returned to normal levels when the nano-extract was used in all treatment modalities.

As shown in Fig. 1, compared to the control group, intoxication with Etn reduced the activity of the AChE enzyme in RBCs and plasma significantly ($p \leq 0.05$). The nano-extract significantly ($p \leq 0.05$) elevated AChE activity compared to the Etn-injected group and restored it to normal levels in RBCs; however, it did not return to normal levels in the plasma of the pre-treated group. Nevertheless, it significantly ($p \leq 0.05$) increased the activity of this enzyme in the post-treated group while restoring its levels in plasma and RBCs back to normal.

3.4. Markers of oxidative stress

According to the data in Table 1, in tissue homogenates (liver and brain), Etn significantly ($p \leq 0.05$) decreased TAC and GSH levels, as well as the activity of the antioxidant enzymes SOD, CAT, and GPx. When compared to the Etn-injected group, the liver tissue of the pre- and post-treated groups exhibited a significant ($p \leq 0.05$) increase in these markers. However, only in the pre-treated group did their levels return to normal. In comparison to the Etn-intoxicated group, all nano-extract treated groups had significantly ($p \leq 0.05$) greater levels of these markers in their brain tissue. However, neither the pre-treated nor post-treated groups of nano-extract were able to return to normal levels.

Rats injected with Etn had significantly ($p \leq 0.05$) higher levels of TPC and LPO than the normal group **(**Fig. 2**)**. The nano-extract significantly ($p \leq 0.05$) decreased the levels of these parameters in both tissues in all nano-extract treated groups when compared to the Etn-intoxicated group. However, the values only returned to normal in the group that received nano-extract before treatment, indicating a stronger ameliorative impact than the group that received post-treatment.

3.5. Inflammatory and fibrotic markers

The quantity of β-amyloid, the activity of the AChE enzyme, and the levels of fibrotic (hydroxyproline) and inflammatory indicators all indicate tissue integrity. The levels of these markers increased as a result of the Etn injection, while AChE activity in the liver tissues decreased significantly ($p \leq 0.05$). The level of the fibrotic marker (hydroxyproline) remained unchanged **(**Table 2**)**. In comparison to the Etn-intoxicated group, the administration of gold nano-extract increased inflammatory markers and lowered AChE activity in both the pre- and post-treated groups, which experienced the same ameliorative impact. AChE enzyme activity decreased, and β-amyloid and inflammatory marker levels increased significantly ($p \leq 0.05$) in brain tissue of the Etn-injected group. The gold nano-extract significantly ($p \leq 0.05$) reduced β-amyloid and inflammatory marker levels compared to the Etn-injected group. This was observed to be associated with increased AChE activity. However, it was unable to restore the levels to normal in any of the treated groups.

3.6. Histopathological examination

In stained liver sections of control rats, as well as gold nano-extract treated rats, light microscopic examination showed normal hepatic parenchymal histoarchitecture **(**Fig. 3**A & B)**. Rats intoxicated with Etn on the other hand, had severe histopathological lesions in their livers that included proliferation of Kupffer cells along with focal hepatocellular necrosis **(**Fig. 3**C)** and fibroplasia, inflammatory cell infiltration in the portal triad **(**Fig. 3**D)**. However, the lesions observed in the livers of rats pre-treated with nano-extract regressed. The examined sections showed only hydropic degeneration of hepatocytes **(**Fig. 3**E)**. Furthermore, the livers of nano-extract post-treated rats exhibited slight Kupffer cell proliferation and a few inflammatory cell infiltrations in the hepatic sinusoids (slight sinusoidal leukocytosis) **(**Fig. 3**F)**. The liver of rats injected with Etn has the greatest adverse effect, as indicated by the scores of the tissue lesions in Supplementary Table 5. The nano-extract exhibited a greater improvement in the pre-treated group than in the post-treated one.

Regarding brain tissue, the control rats as well as rats treated with nano-extract displayed normal architecture with intact neurons in the cerebral cortex **(**Fig. 4**A & B)**. In contrast, in Etn intoxicated rats, remarkable neuropathic alterations were seen in the cerebral cortex. The examined sections revealed shrunken, dark pyknotic neurons **(**Fig. 4**C & D)**, cellular edema **(**Fig. 4**C)**, vacuolation of neuropil and neuronophagia **(**Fig. 4**D)**. Meanwhile, the cerebral cortex was markedly improved in nano-extract pre-treated rats, along with regression of the neuropathic damage characterized by sparse necrosis of neurons and slight vacuolation of neuropil **(**Fig. 4**E)**. Furthermore, the cerebral cortex displayed necrosis of some neurons with vacuolation of neuropil in the post-treated group **(**Fig. 4**F)**. Compared to the control group, histopathological scores of the brain tissue lesions, as shown in Supplementary Table 6, indicated statistically significant ($p \leq 0.05$) alterations in the Etn-injected group. The nano-extract showed greater amelioration in the pre-treated group than in the post-treated group.

3.7. Electrophoretic assays

3.7.1. Protein pattern

Native protein pattern in liver tissue revealed that four normal bands were hidden by two characteristic (abnormal) ones (Rfs 0.30 and 0.74; Int. 203.34 and 181.00; B% 14.91 and 12.43, respectively) in the Etn-injected group, indicating physiological changes. Therefore, the SI value (SI = 62.50 %) dropped when compared to the normal group **(**Fig. 5**a)**. In the nano-extract pre-treated group, the protein pattern was improved by restoring four normal bands (Rfs 0.24, 0.33, 0.43 and 0.68;

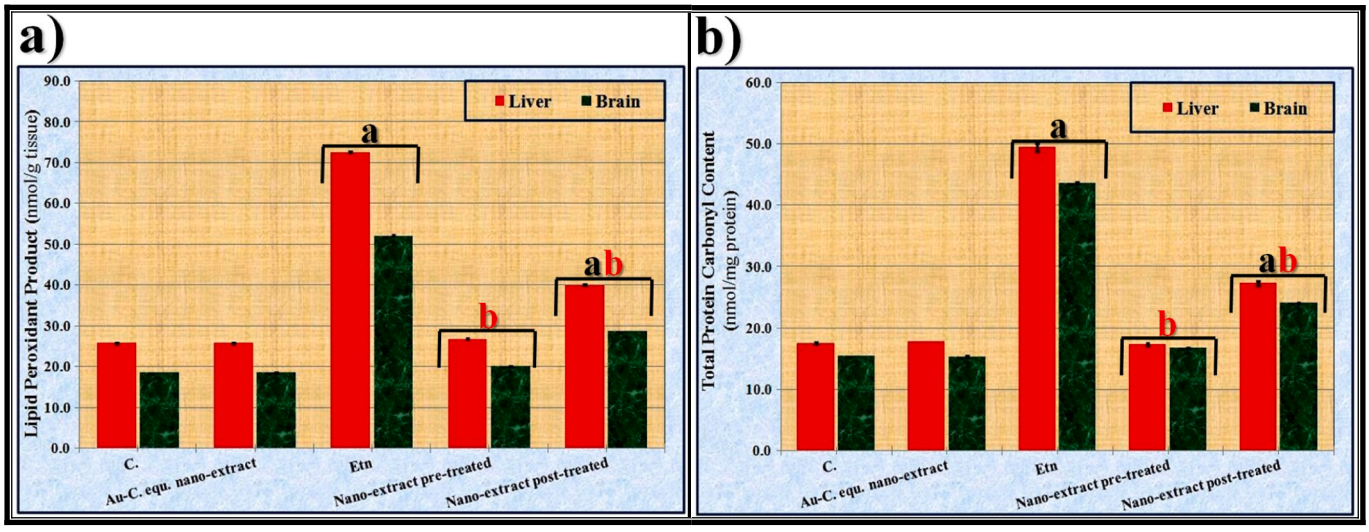

Fig. 2. Effect of the *C. equisetifolia* gold nano-extract against the changes in **a)** lipid peroxidation product, and **b)** total protein carbonyl content induced by ethion (Etn) in both liver and brain tissues of rats. Data were presented as mean ± SE (from five replicates). **a**: Indicates significance at $p \leq 0.05$ compared to the control and **b**: to Etn injected group.

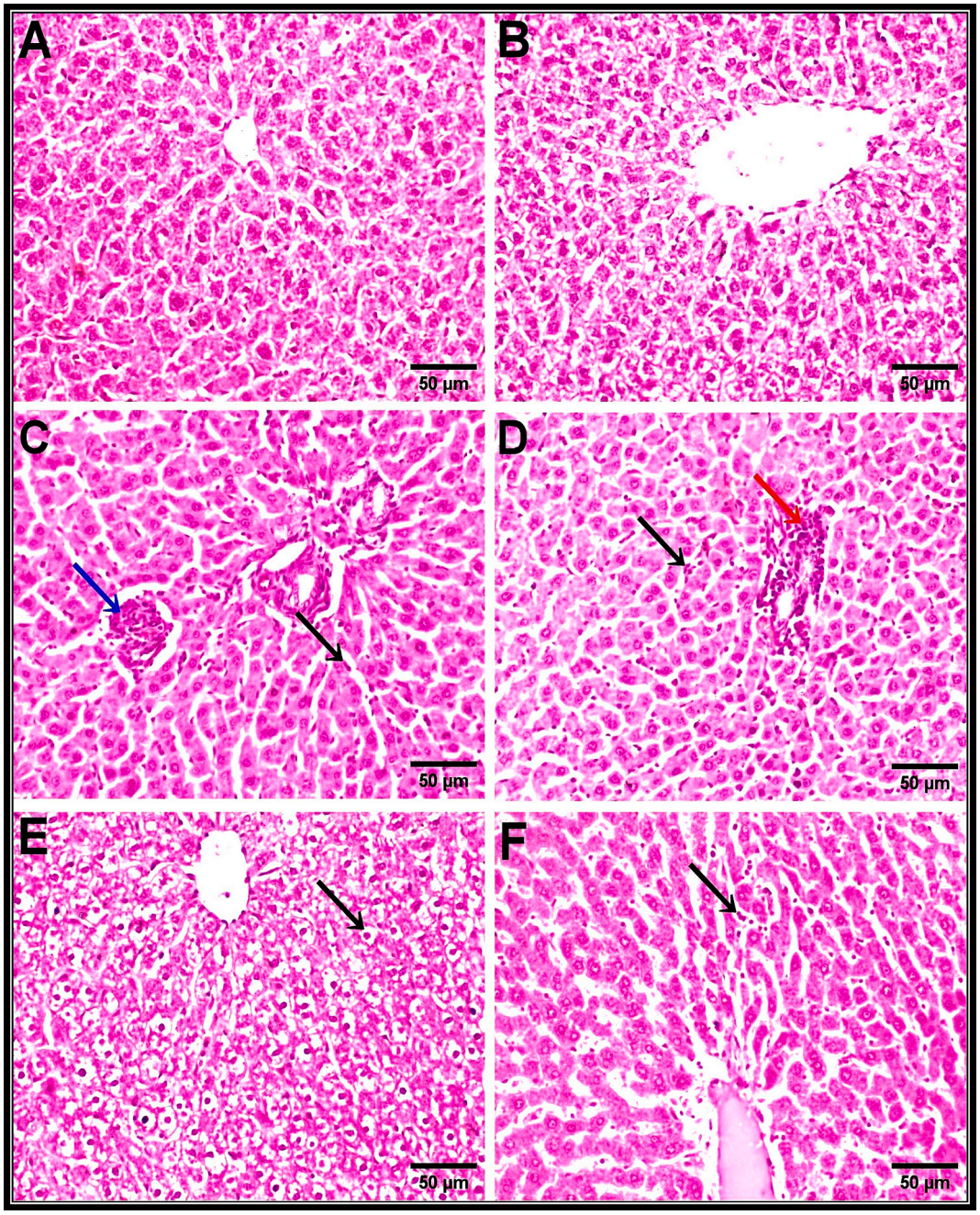

Fig. 3. Photomicrographs of the stained liver sections of rats (Scale bar 50 µm), **(A)** normal control & **(B)** Gold nano-extract treated group showing normal histoarchitecture of hepatic parenchyma. **(C) & (D)** Etn-injected group showing Kupffer cells proliferation (black arrow), focal hepatocellular necrosis associated with inflammatory cells infiltration (blue arrow), inflammatory cells infiltration in the portal triad (red arrow). **(E)** The gold nano-extract pre-treated group showing hydropic degeneration of hepatocytes (arrow). **(F)** The gold nano-extract post-treated group showing slight sinusoidal leukocytosis (arrow).

Int. 139.11, 182.00, 157.00 and 181.00; B% 9.22, 11.50, 10.22 and 11.08, respectively) while hiding the abnormal ones. Slight ameliorative effect was noticed in the nano-extract post-treated group by hiding the abnormal bands and restoring only 3 ones (Rfs 0.24, 0.33 and 0.68; Int. 140.00, 181.00 and 173.89; B% 10.40, 12.50 and 11.66, respectively). The pre- and post-treated groups are 100.00 and 94.12 %, respectively, closer to the control group at the physiological state.

The protein pattern of the brain tissue showed that four normal bands are missing, while two abnormal ones (Rfs 0.27 and 0.48; Int. 220.00 and 184.11; B% 19.40 and 18.78, respectively) are present in the Etn-injected group indicated physiological changes. Therefore, compared to the control group, this group had the lowest SI value (SI = 50.00 %) (Fig. 5**b**). By concealing the aberrant bands and restoring four normal bands (Rfs. 0.08, 0.19, 0.34, and 0.85; Int. 186.00, 190.00, 216.34, and 214.00; B% 12.43, 13.47, 13.89, and 14.38, respectively), the nano-extract improved the protein pattern in the pre-treated group. As a result, the pre-treated group's SI value reaches its maximum value (SI = 100.00 %) compared to the normal group. Since the nano-extract only concealed one aberrant band and restored one normal band (Rf 0.20; Int. 185.11; B% 17.51), the post-treated group showed a lesser ameliorative effect. There was a 66.67 % qualitative similarity between this treated group and the control.

3.7.2. Lipid moiety of protein pattern

In the liver tissue, this pattern revealed that one characteristic band (Rf 0.80; Int. 246.11; B% 20.08) obscured two normal bands in the Etn-

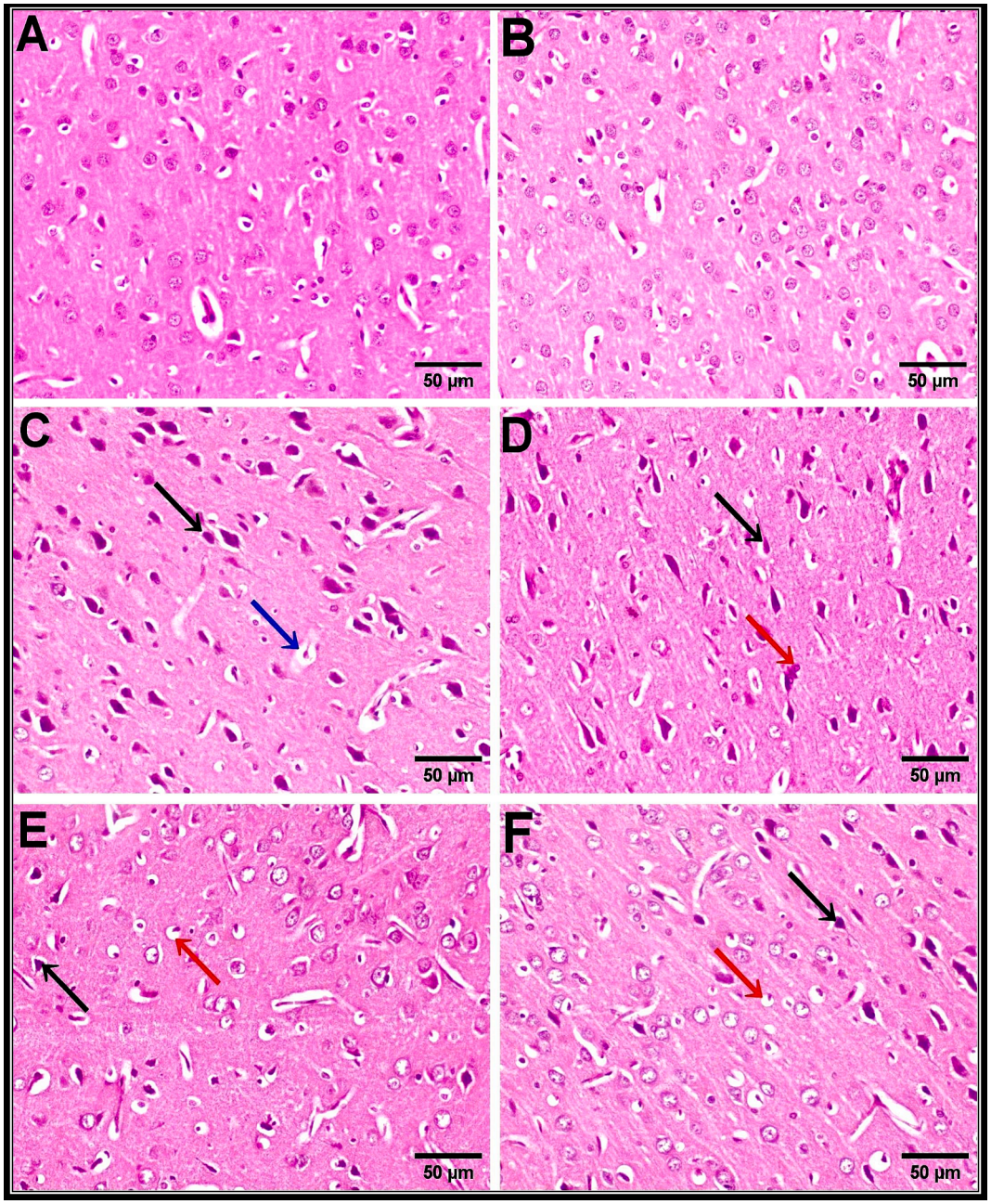

Fig. 4. Photomicrographs of the stained cerebral cortex of rats (Scale bar 50 µm), **(A)** control & **(B)** Gold nano-extract treated group showing the normal histological architecture with intact neurons. **(C) & (D)** Etn-injected group showing shrunken, dark pyknotic neurons (black arrow), neuronophagia (red arrow) and cellular edema (blue arrow). **(E)** The gold nano-extract pre-treated group showing sparsely necrosis of neurons (black arrow) and vacuolation of neuropil (red arrow). **(F)** The gold nano-extract post-treated group showing necrosis of some neurons (black arrow) and vacuolation of neuropil (red arrow).

injected group, indicating qualitative alterations. There is a 72.73 % physiological similarity between this group and the control group (Fig. 5**a**). Normal bands that were previously absent are now restored (Rfs 0.12 and 0.75; Int. 187.00 and 224.78; B% 15.38 and 13.82, respectively), while the aberrant band is enhanced. The protein pattern is improved in the nano-extract pre-treated group. While the unique band vanished, only one normal band (Rf 0.75; Int. 219.11; B% 21.02) was recovered in the post-treated group, indicating a minor ameliorative impact. The pre- and post-treated groups were qualitatively similar to the control by 100.00 and 80.00 %, respectively.

In the brain tissue, this native pattern revealed that one band was missing due to the Etn injection. As a result, the Etn-injected group was 85.71 % physiologically identical to the normal group (Fig. 5**b**). The pattern was identical to the control rats (SI = 100.00 %) after the gold nano-extract pre-treatment restored the missing band (Rf 0.66; Int. 161.44; B% 17.17). Nevertheless, the native pattern in the post-treated group was not improved by the nano-extract. As a result, this group and the control group shared 85.71 % of the same physiological characteristics as the group that received the Etn injection.

3.7.3. Calcium moiety of protein pattern

This native pattern showed that the Etn-injection caused physiological abnormalities in the liver tissue identified by replacing two normal bands with two characteristic bands (Rfs 0.30 and 0.77; Int. 132.00 and 132.00; B% 23.41 and 23.89, respectively). Theerefore, the physiological similarity between the Etn-injected group and the control group decreased by 50.00 % (Fig. 5**a**). By restoring the two missing normal bands, Rfs 0.18 and 0.70, in the pre- (Int. 132.00 and 116.89; B% 21.78

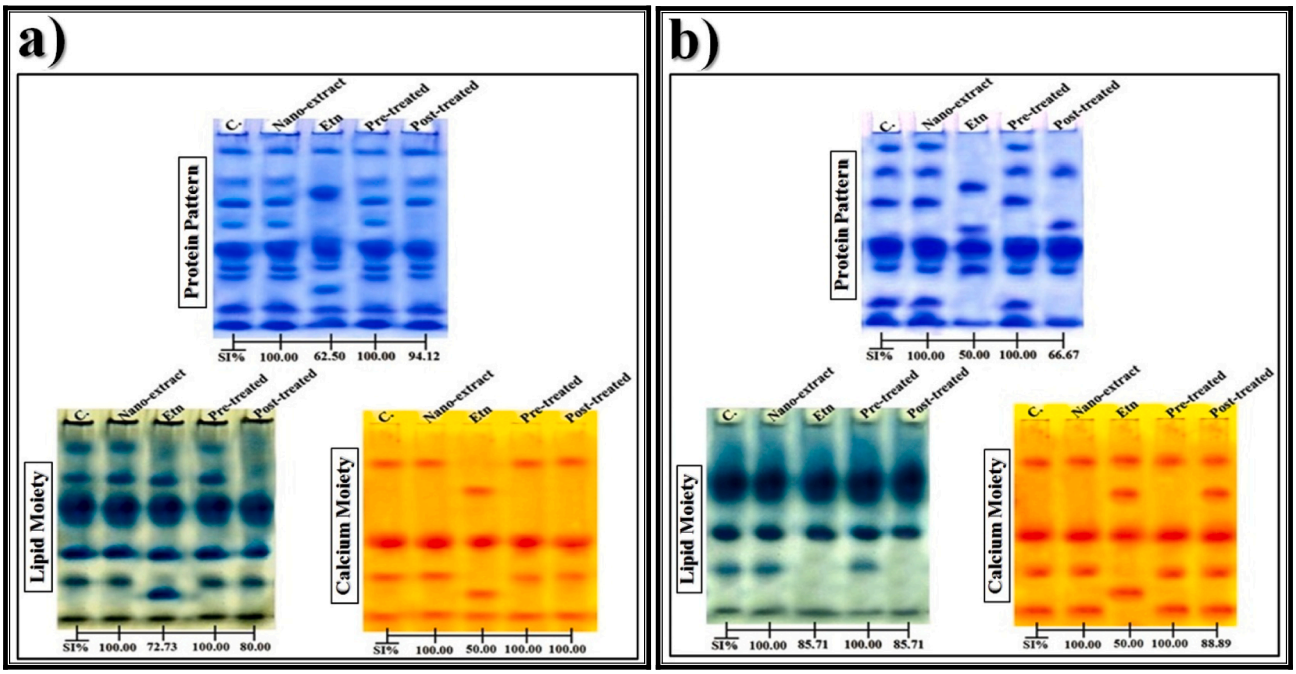

Fig. 5. Effect of the *C. equisetifolia* gold nano-extract against the physiological alterations induced in the native protein patterns by ethion (Etn) in **a)** liver, and **b)** brain tissues of rats.

and 21.21, respectively) and post-treated groups (Int. 132.00 and 118.67; B% 25.18 and 23.65, respectively), both the pre- and post-treated groups showed the same ameliorative effect from the nano-extract, which was physiologically equal to the control group (SI = 100.00 %).

In the brain tissue, the native pattern showed that one characteristic band (at Rf 0.82; Int. 149.00; B% 24.63) was present in the group that received Etn injection, obscuring two normal bands and giving rise to two aberrant ones (Rfs 0.35 and 0.82; Int. 148.00 and 149.00; B% 24.25 and 24.63, respectively). The physiological similarity of the Etn-injected group was 50.00 % lower than that of the control group **(**Fig. 5**b)**. By restoring the missing (normal) bands (Rfs 0.73 and 0.90; Int. 148.00 and 148.00; B% 23.76 and 21.90, respectively) and hiding the aberrant ones in the pre-treated group, which was qualitatively comparable to the control (SI = 100.00 %), the gold nano-extract significantly improved this native pattern. The post-treated group showed a slight improvement, with only one aberrant band remaining hidden and the missing (normal) bands (Rfs 0.73 and 0.90; Int. 146.00 and 148.00; B% 19.63 and 17.27, respectively) restored. As a result, this group was 88.89 % qualitatively identical to the normal group.

3.7.4. Catalase (CAT) pattern

In the liver tissue, the isoenzyme pattern revealed that the presence of one abnormal band (Rf 0.31; Int. 126.67; B% 24.66) and obscuring the CAT3 type in the Etn-injected group indicate qualitative alterations. Comparing the Etn-injected group to the control group, the physiological similarity decreased to 75.00 % **(**Fig. 6**a)**. Returning the missing normal (CAT3) type (Rf 0.75; Int. 134.67; B% 20.38) greatly improved this isoenzyme pattern, while hiding the aberrant one in the pre-treated group, making it 100.00 % more physiologically similar to the control. In the post-treated group, the nano-extract showed no improvement. Consequently, it maintained a 75.00 % resemblance to the control (as in the Etn-injected group).

In the brain tissue, the Etn-injected group showed one aberrant band (Rf 0.36; Int. 130.22; B% 23.12), indicating physiological changes. Comparing the Etn-injected group to the control group, the physiological similarity dropped to 85.71 % **(**Fig. 6**b)**. By eliminating the abnormal band in all therapy modalities, the gold nano-extract exhibited an equivalent degree of enhancement. As a result, their biological similarity to the control group was 100.00 %.

3.7.5. Peroxidase (POX) pattern

In the liver tissue, the isoenzyme pattern showed that two unique (abnormal) bands (Rfs 0.18 and 0.64; Int. 134.67 and 136.44; B% 13.52 and 13.69, respectively) and the absence of two normal POX types (POX1 and POX3) were indicative of the qualitative changes in the Etn-injected group. The Etn-injected group's physiological resemblance to the control group decreased to 66.67 % **(**Fig. 6**a)**. The restoration of the two absent POX types (POX1 and POX3) observed at Rfs 0.12 and 0.43 (Int. 135.56 and 132.89; B% 14.12 and 13.23, respectively) and hiding the abnormal bands in the pre-treated group, resulting in complete similarity to the control (SI = 100.00 %), helped alleviate the negative effects of Etn injection. Only one normal POX type (POX1) was restored, leading to a slight improvement in the isoenzyme pattern (Rfs 0.12; Int. 139.11; B% 15.02). The anomalous bands were masked in the post-treated group, achieving a 90.91 % physiological similarity to the control.

In the brain tissue, the isoenzyme pattern revealed that by hidding the POX1 and POX3 types, the isoenzyme pattern depicted the physiological alterations in the Etn-intoxicated group. Consequently, this group had the lowest SI value (SI = 80.00 %) compared to the normal group **(**Fig. 6**b)**. Restoring the two missing POX types (POX1 and POX3) (Rfs 0.13 and 0.44; Int. 189.00 and 187.00; B% 15.47 and 14.88, respectively) in the pre-treated group reduced the negative impact caused by Etn intoxication. At the physiological level, this restoration returned the levels to 100.00 % of those of the control group. The abnormal band was hidden, and only one normal POX type (POX1) (Rf 0.12; Int. 184.00; B% 17.50) was restored in the post-treatment group, indicating a slight decrease. As a result, this group and the control group shared 90.91 % of their physiological characteristics.

3.7.6. α-Amylase (α-Amy) pattern

In the liver tissue, the isoenzyme pattern showed that changes in the pattern were observed in the Etn-injected group, where the second α-Amy type (α-Amy2) was absent, and two abnormal bands appeared with characteristic Rfs of 0.44 and 0.89, Int. of 132.00 and 141.00, and B

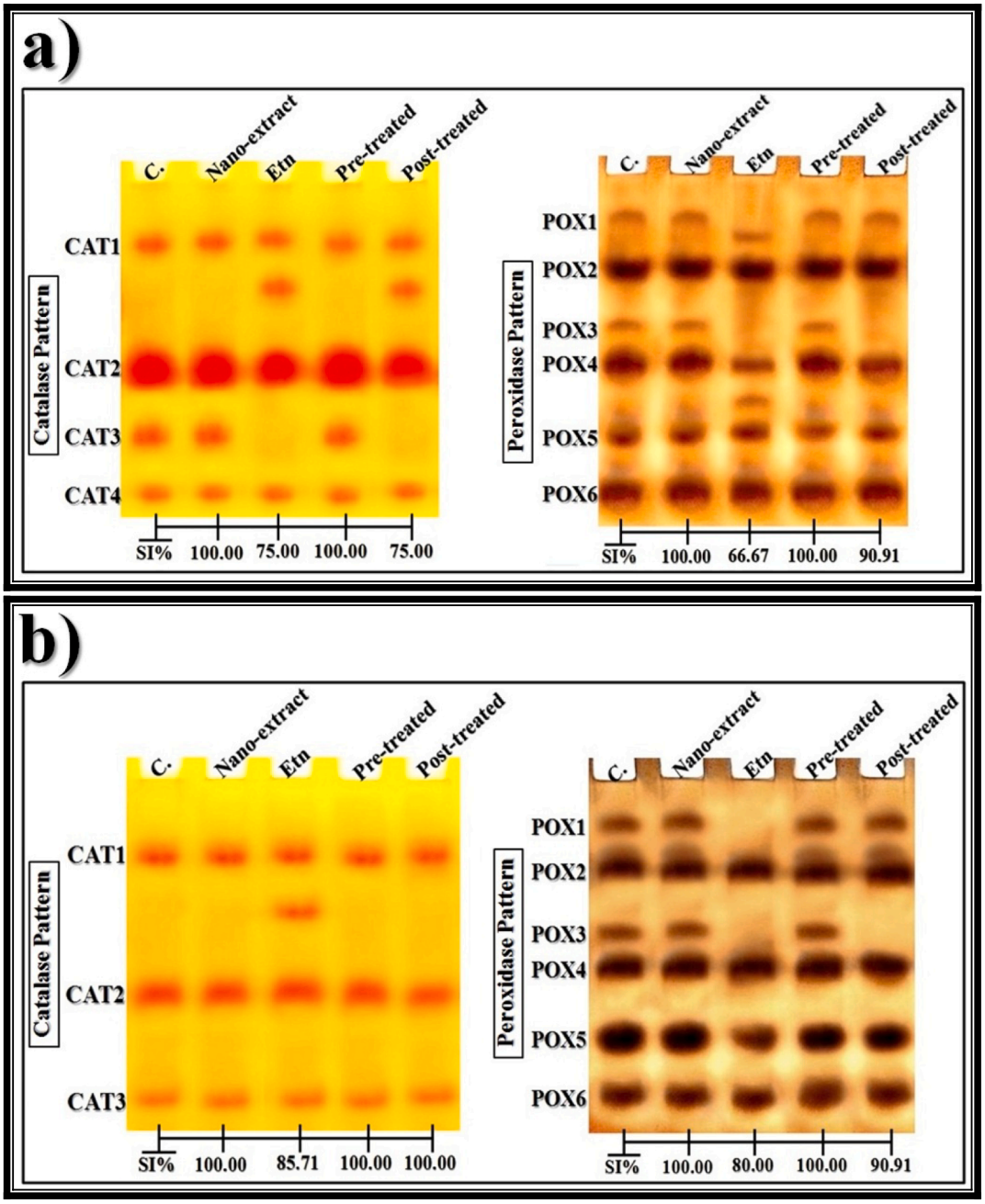

Fig. 6. Effect of the *C. equisetifolia* gold nano-extract against the physiological alterations induced by ethion (Etn) in the electrophoretic antioxidant isoenzymes patterns in **a)** liver, and **b)** brain tissues of rats.

% of 32.72 and 33.76, respectively. Consequently, this group had the lowest SI value (SI = 40.00 %) with respect to the normal group **(**Fig. 7**a)**. By restoring the missing α-Amy2 at Rf 0.67 in both the pre-treated (Int. 157.00 and B% 51.58) and post-treated (Int. 155.22 and B% 52.30) groups, along with the removal of the abnormal bands, the nano-extract improved the isoenzyme pattern to the same extent in all therapy approaches. The pre- and post-treated groups were therefore identical to the normal group, with a physiological SI level of 100.00 %.

The isoenzyme pattern in the brain tissue showed no physiological or quantitative changes were identified in the Etn injected group **(**Fig. 7**b)**. After the administration of the nano-extract, neither the pre-treated nor post-treated groups showed any electrophoretic alterations, and their physiological characteristics were 100.00 % identical to the normal group.

3.7.7. Esterase (EST) pattern

In the liver tissue, the α-EST isoenzyme pattern revealed that an abnormal band (Rf 0.83; Int. 116.00 and B% 30.01) appeared along with the disappearance of one α-EST type (α-EST2) due to qualitative changes in the isoenzyme pattern caused by the Etn injection. As a result, the physiological similarity of this group to the control group decreased to 80.00 % **(**Fig. 7**a)**. The isoenzyme pattern improved in the pre-treated group as the aberrant band vanished and the normal (α-EST2) type that had been missing was restored (Rf 0.31; Int. 116.89 and B% 30.56). As a result, there was a 100.00 % qualitative resemblance between the isoenzyme pattern and the control group. The abnormal band was not restored in the post-treated group's isoenzyme pattern, indicating only a minor improvement. This group and the normal group had an 80.00 % physiological similarity.

In the brain tissue, the isoenzyme pattern of the Etn-injected group

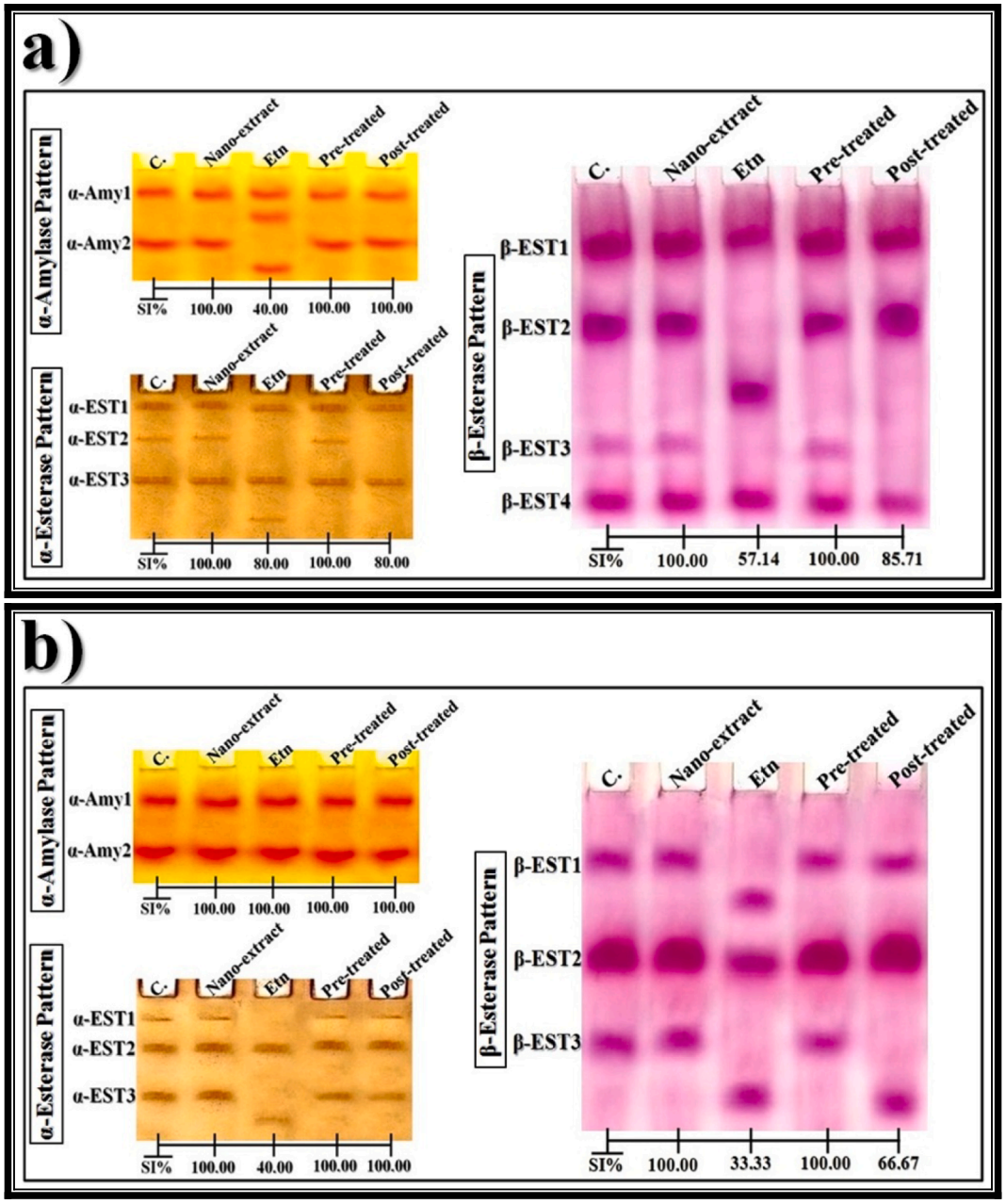

Fig. 7. Effect of the *C. equisetifolia* gold nano-extract against the physiological alterations induced by ethion (Etn) in the different electrophoretic isoenzymes patterns in **a)** liver, and **b)** brain tissues of rats.

showed qualitative changes, with two α-EST types (α-EST1 and α-EST3) buried and one characteristic (abnormal) band (Rf 0.83; Int. 98.18; B% 48.22) being noticeable. At the qualitative level, this group showed the lowest SI value (SI = 40.00 %) in comparison to the normal group (Fig. 7**b)**. The same improvement was achieved by the nano-extract, which concealed the abnormal band and restored the missing (normal) types (α-EST1 and α-EST3) at Rfs 0.13 and 0.68 in both the pre-treated (Int. 113.00 and 129.34; B% 30.76 and 34.93, respectively) and post-treated groups (Int. 114.89 and 119.56; B% 28.06 and 28.55, respectively). At the qualitative level, the pre- and post-treated groups (SI = 100.00 %) were identical to the healthy group.

In the liver tissue, the β-EST isoenzyme pattern revealed that the appearance of one unique band (Rf 0.59; Int. 98.00; B% 35.18) and the elimination of two normal types (β-EST2 and β-EST3) were indicators of the physiological alterations in the Etn-injected group. Consequently, this group's physiological similarity to the normal group was the lowest (SI = 57.14 %) (Fig. 7**a)**. By concealing the anomalous band and reinstating the absent β-EST2 and β-EST3 types (Rfs 0.40 and 0.76; Int. 198.00 and 116.89; B% 27.74 and 19.27, respectively) in the pre-treated group, the isoenzyme pattern was improved. This resulted in a physiological pattern that was identical to that of the normal rats (SI = 100.00 %). In the post-treated group, the aberrant band disappeared and only one normal type (β-EST2) was restored (Rf 0.38; Int. 198.89; B% 37.70), which improved the isoenzyme pattern significantly and rendered the group qualitatively equivalent to the control group by 85.71 %.

In the brain tissue, the isoenzyme pattern showed that the Etn injection caused physiological changes, as evidenced by the appearance of two aberrant bands (Rfs 0.30 and 0.84; Int. 167.67 and 176.56; B% 32.81 and 33.91, respectively) and the disappearance of two normal types (β-EST1 and β-EST3). As a result, in comparison to the control group, this group had the lowest SI value (SI = 33.33 %) (Fig. 7**b)**. The nano-extract significantly improved the isoenzyme pattern in the pre-

treated rats by restoring the missing β-EST1 and β-EST3 types (Rfs 0.19 and 0.69; Int. 160.56 and 164.11; B% 28.46 and 27.84, respectively). As a result, at a qualitative level, the isoenzyme pattern totally resembled that of the normal group (SI = 100.00 %). Only one aberrant band disappeared, and only one normal type (β-EST1) (Rf 0.20; Int. 167.67 and B% 29.88) was restored in the post-treated group, indicating a small improvement in the isoenzyme pattern. Consequently, this group's resemblance to the control group dropped to 66.67 %.

3.8. Molecular assay

The relative expression of the Bcl2 gene declined, while the expression of the BAX, p^{53}, and Caspase-3 genes significantly ($p \leq 0.05$) increased in the target tissues (liver and brain) of the Etn-injected group with respect to the normal rats (Fig. 8). The nano-extract significantly ($p \leq 0.05$) increased the expression of the Bcl2 gene while decreasing the relative expression of the BAX, p^{53}, and Caspase-3 genes in all nano-extract treated rats compared to the Etn-intoxicated rats. However, the decreased relative expressions of apoptotic genes did not return to normal values in all treated groups.

4. Discussion

The current study demonstrated that Etn injection significantly reduced body weight gain. This was in line with **Campana *et al.***,[59] who showed that exposure to ethion caused changes in morphology and symptoms. This may be linked to the neurological abnormalities in rats given Etn injections as well as distinctive alterations in the activity of the AChE enzyme, which causes the buildup of acetylcholine to activate cholinergic receptors. The group that received Etn injections showed a significant increase in relative liver and brain weights. This might be a sign of abnormalities in eating capacity and, consequently, metabolic pathway function.[60] In comparison to the Etn-intoxicated group, the body weight gain was higher in the nano-extract pre-treated group. This might be explained by better glycemic and lipid management, which was boosted when Au-NPs were present.[61] Additionally, the increase in body weight gain after the administration of the gold nano-extract may be due to the presence of phenolic (active) chemicals, which can improve antioxidant activity and increase food intake and growth rate.[62]
.

OPs are known to induce apoptosis and damage DNA in spleen and bone marrow cells. Consequently, they have a direct impact on the blood cells.[63] Red blood cell indices were found to have dropped in the Etn-injected group, which is consistent with the hypothesis of **Mohammod Mostakim *et al.***,[64] who demonstrated that the decrease in the RBC count could be caused by the hematopoietic tissue's incapacity to release normal RBCs into the blood circulation, increasing erythrocyte destruction in the hematopoietic organ, osmoregulatory dysfunction, or inhibition of erythropoiesis. Furthermore, the development of a hypoxic state and the low Hb content of the circulatory system may potentially be connected to the notable decline in these indices' values.[65] WBCs are in charge of immunological responses and defensive processes.[66] During the experiment, it was observed that the group that received the Etn injection had fewer differential white blood cells than the control group. As shown by **Deabes *et al.***,[67] it is well known that OPs cause lymphopenic leucopenia by destroying leukocytes as a result of increased ROS generation, which raises peroxidation products. The gold nano-extract was able to restore the levels of these measurements to normal because of the efficacy of the polyphenolic compounds, which can scavenge the generated ROS and help convert iron from the ferrous to the ferric state. As a result, they increase iron absorption and, therefore, the integrity of red and white blood cells that have been weakened by

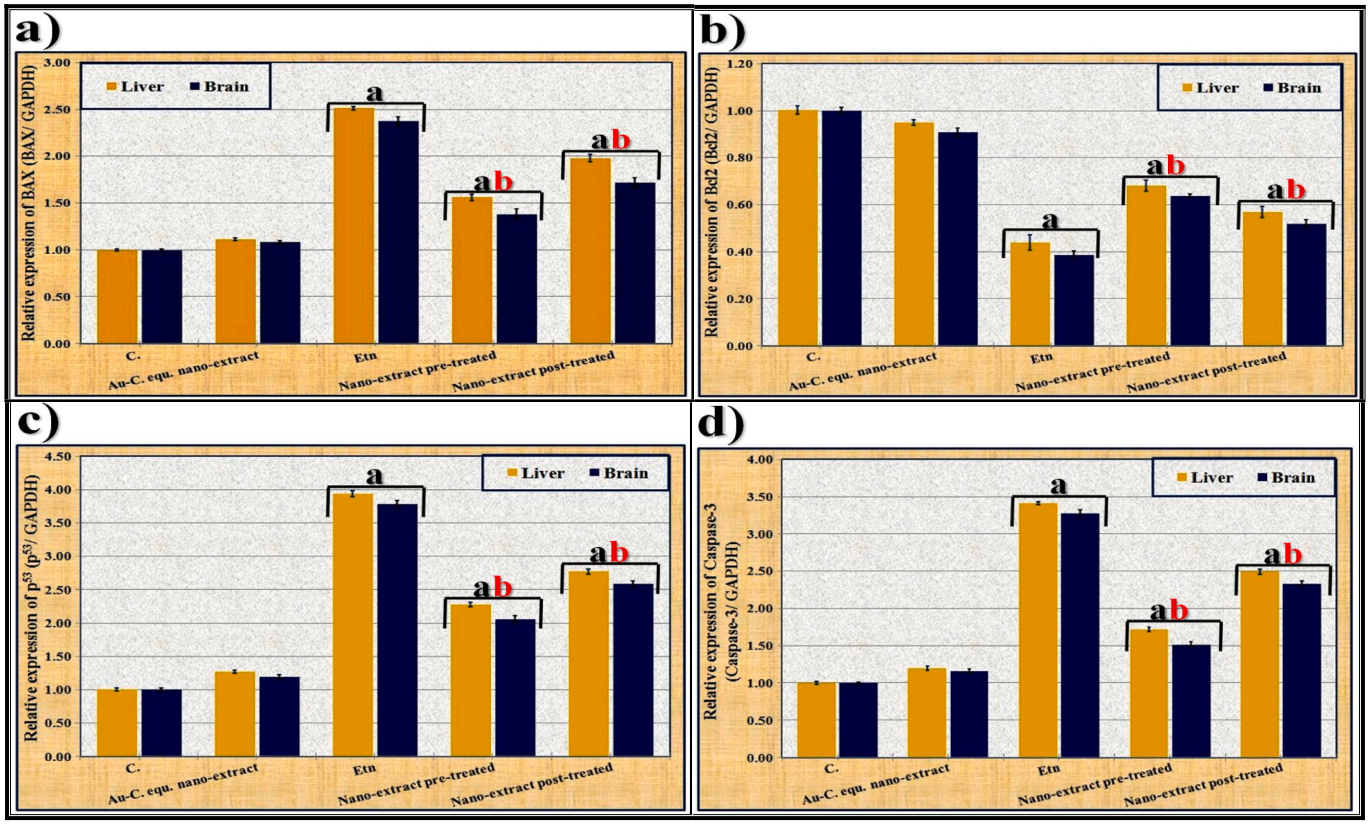

Fig. 8. Effect of the C. equisetifolia gold nano-extract against the molecular changes induced by ethion (Etn) in the relative expression of apoptotic genes a) BAX, b) Bcl2, c) p^{53}, and d) Caspase-3 genes induced by ethion (Etn) in both liver and brain tissues of rats. Data were presented as mean ± SE (from five replicates). a: Indicates significance at $p \leq 0.05$ compared to the control and b: to Etn injected group.

oxidative stress brought on by OPs.[68] Furthermore, the secondary metabolites' capacity to prevent platelet death and encourage platelet formation resulted in an increase in the platelet count. Furthermore, they preserved the integrity of platelet membranes by reducing the synthesis of lipid peroxides inside them.[69] .

AChE inhibition is one of the main mechanisms of OP toxicity. One important enzyme that affects brain function is AChE.[70] The AChE enzyme's blood activity dropped in the rats given ethanol during the current investigation. This is explained by the OPs' capacity to phosphorylate the serine-OH group of AChE, permanently inhibiting the enzyme. Acetylcholine thus accumulated in synapses and was unable to be released from presynaptic membranes, inhibiting nerve impulse conduction and causing cholinergic pathways to become hyperactive.[71] Due to the antioxidant properties of the phenolic phyto-constituents, which have a moderating effect on the AChE enzyme activity, the administration of gold nano-extract enhanced the activity of the AChE enzyme in both the plasma and RBCs compared to the Etn-intoxicated rats.[72] Furthermore, **Bekheit *et al.***[73] proposed that adding Au-NPs to plant extracts improved the biological efficacy of phenolic compounds.

According to **Kunnaja *et al.***,[74] blood measurements were used to evaluate the physiological and pathological conditions of an animal's critical organs. The most active metabolizing organ required to effectuate thiono-organophosphate bioactivation is believed to be the liver.[75] Throughout the current investigation, the liver enzyme activity in the sera of the group that received Etn injections significantly rose. This rise may be related to the toxicant's overproduction of ROS and oxidative stress, which could eventually result in liver damage and necrosis, leading to damage in cell membranes and leakage of enzymes into the circulation. Consequently, these enzymes are released from hepatic cells and found in the blood.[76] In the sera of rats given Etn injection, TP and albumin levels decreased, while levels of the nitrogenous product (urea, creatinin, and uric acid) significantly increased after exposure to Etn. This may be related to oxidative damage to the kidneys caused by increased ROS generation and decreased antioxidants.[77] The liver, where there is a reduction in protein synthesis, digestion, and absorption, is the primary organ affected by this OP chemical. On the other hand, glomerular filtration insufficiency caused a drop in TP and albumin levels, leading to decreased excretion and increased serum levels.[78] .

Abnormal uric acid net reabsorption in the proximal tubules may also be linked to changes in uric acid levels.[79] Along with lipid measurements in the sera of the rats given Etn injections, it was noticed that the cardiac enzymes (CK and LDH) were raised in relation to heart activities. This may have something to do with oxidative stress brought on by an overabundance of ROS.[80–81] Furthermore, the findings showed that the Etn-injected group's serum had higher levels of TGs and cholesterol. This could be because the OP blocked the bile duct, which reduced the amount of cholesterol secreted into the intestine,[82] or because it inhibited pancreatic function, resulting in poor lipid absorption.[83] .

The gold nano-extract contained secondary metabolites that could block the activities of transaminases, enabling it to alleviate the toxicity caused by OPs in the liver, kidneys, and heart tissues.[84] Additionally, the presence of Au-NPs enhances the integrity of hepatocyte membranes, preventing the leakage of these enzymes.[85] The ability of Au-NPs to enhance the integrity and regenerative capacity of renal tubules may explain the normalization of renal measurement levels by the gold nano-extract.[86] Due to its hypolipidemic qualities, the administration of the nano-extract restored lipid measures and cardiac enzyme levels to normal. The phytochemicals' ability to inhibit fatty acid oxidation due to their antioxidant activity may be the cause of this impact. This suggests that the gold nano-extract has hypolipidemic qualities, which in turn lead to a decrease in cardiac enzymes.[87]

During the current study, hepatic and brain tissues showed higher levels of peroxidation products (LPO and TPC), and enzymatic and non-enzymatic antioxidants were found to be depressed, affecting antioxidant system indicators. This result is consistent with that of **Saoudi *et al.***,[88] who demonstrated that exposure to OPs leads to changes in antioxidants and the generation of oxidative stress. An imbalance between the biological system's capacity to detoxify reactive intermediates and the systemic generation of ROS leads to oxidative stress. Consequently, DNA and other vital biomolecules may be destroyed as a result of high ROS generation, as well as the initiation of lipid peroxidation.[89] The gold nano-extract reversed the adverse effects of Etn injection and restored antioxidant system measures in these target tissues. This was explained by the methanolic *C. equisetifolia* extract's alkaloids, polyphenolics, saponins, and glycosides. The biosynthesized Au-NPs were responsible for the antioxidant activity and the potential ameliorative effects of the nano-extract.[90] Levels of LPO and TPC decreased following treatment with nano-extract because phyto-constituents can block xanthine oxidase or scavenge the reactive metabolites that induce lipid peroxidation.[91] Furthermore, **Shahmahmoodi *et al.***[92] suggested that the biosynthesized Au-NPs might adsorb some ethion and reduce its harmful effects. The surface area of the nanoparticles, which increases as particle size decreases, was linked to their ability to absorb more toxicants.

Pro-inflammatory cytokine levels were higher in the liver and brain tissues of the Etn-intoxicated group in the current study. This increase may be associated with increased immunological response, T-cell proliferation, and lymphocyte activation.[93] Additionally, OPs mediate mitochondrial oxidative stress, which triggers the inflammasome and the innate immunological response that follows. Consequently, ROS scavengers can help heal the lesions caused by OPs.[94] The decrease in AChE activity in the target tissues (liver and brain) of rats given Etn may be related to a lowering rate of enzyme synthesis due to insufficient glucose permeation across the surface membrane or to the inhibition of enzyme synthesis caused by the changed cellular environment in the brain.[95] The inflammation induced by the Etn injection was reduced by the treatment with gold nano-extract. This supports the findings of **El-Feky and Aboulthana**,[96] who stated that the extract's anti-inflammatory qualities are made possible by its active phyto-constituents. Furthermore, the Au-NPs can interact with IL-6 extracellularly, which disrupts the transmission of inflammatory signals. The aggregation around Au-NPs not only slows the evolution of the inflammatory response but also prevents IL-6 from binding to cellular receptors.[97] .

According to histopathological examinations, the brain and liver are the organs most vulnerable to OP buildup.[98] **Badr**[8] stated that Etn is metabolized in the liver and transformed into more reactive products, leading to the formation of various reactive species. The current study showed that Etn intoxication caused significant histopathological abnormalities in liver tissue. The hepatotoxic effects of these reactive metabolites are evident from the drastic changes they induce in hepatic tissues.

Due to the inhibitory effects of antioxidant enzymes and the excessive production of ROS, Etn injection caused significant disruptions in brain tissues, resulting in degeneration of Purkinje cells in the cerebellum and injury to neurons in the cerebral cortex.[10,99] According to **Abdel-Salam *et al.***,[80] these OPs are lipophilic, which facilitates their absorption and passage over the blood–brain barrier into the central nervous system. Damage to the neurological system and oxidative injury-induced neuronal degeneration hampered neural conduction. The histopathological alterations brought on by Etn injection were lessened by administering nano-extract. Due to their ability to maintain membranes by donating hydrogen atoms, phenolic compounds that exhibit antioxidative actions may be responsible for this.[100] The antioxidant, radical scavenging, and anti-inflammatory properties of the active components are enhanced in the presence of Au-NPs, leading to a decrease in histopathological damage scores. Consequently, leukocyte migration and macrophage infiltration are reduced.[101] .

Physiological variations in protein and isoenzyme patterns are detected by electrophoresis and manifest as either the appearance of

abnormal bands or the disappearance of normal ones.[102] The fraction of the SI that represents the tissue's physiological state fluctuates because of qualitative shifts.[72] The present study found that native protein patterns in the target tissues were qualitatively altered by the Etn injection. This may involve how the OPs restrict the expression of certain genes or promote the synthesis of specific mRNAs by other genes, leading to the production of stress-induced proteins.[103] Additionally, the appearance of new (abnormal) protein bands in the examined tissues of rats injected with Etn may be attributed to the inhibition of protein anabolic activities or the denaturation of various proteins, resulting in alterations in the structural conformations of functional proteins and, consequently, cytoplasmic proteins.[104] The decrease in AChE activity, which subsequently affects catecholamines, could be associated with changes in the native protein composition. In rats receiving Etn injections, the catecholamines may cause glycogenolysis and consequent hyperglycemia, which would lead to protein glycosylation.[105] The chaperone in charge of protein folding is less efficient as a result of the glycation process.[106] In rats receiving Etn injection, the lipid moiety of protein pattern undergoes physiological changes due to oxidative modifications caused by excessive ROS production in the lipid portion.[107] The calcium moiety of protein pattern shows both qualitative and quantitative anomalies as a result of Etn intoxication, leading to an increase in calcium concentration. These biomolecules are affected by increased ROS production and oxidative stress.[52,108] .

The degeneration of protein contents caused by unrestrained ROS production affected the CAT and POX isoenzyme patterns in the liver and brain of the Etn-injected rats. This may have led to alterations in the physico-chemical makeup of the endogenous CAT and POX enzymes.[109] Furthermore, the glycosylation process of tissues is accelerated by catecholamine accumulation and AChE enzyme inhibition.[110] Hormonal and metabolic changes may be responsible for the changes in the α-amylase isoenzyme caused by the Etn injection.[111] The fractional activity of the protein caused by DNA damage has changed as a result of oxidative changes, which in turn impact the rate of protein expression.[102] The distinctive alterations in the α- and β-EST isoenzymes in rats exposed to Etn may be linked to OPs' function in blocking the esterase enzymes due to irreversible covalent formation.[105] The abnormal EST pattern was caused by an excess of ROS that impaired the stability of the protein molecule through sulfhydryl-mediated cross-linking of labile amino acids.[112] Different isoenzymes' fractional activity is altered by oxidative stress and excessive ROS generation as they slow down the rate at which proteins are produced following DNA damage.[113]

The physiological alterations caused in the livers and brains of the rats given Etn were lessened by the administration of a gold nano-extract from *C. equisetifolia*. All natural protein and isoenzyme patterns showed this. The scavenging action of the active (phenolic) phyto-constituents, which can protect these physiologically active macromolecules from oxidative stress, is responsible for this effect.[72] According to **Aboulthana *et al.***,[29] the inclusion of active components with lipolytic activity and lipolysis-stimulating compounds reduced the anomalies caused by the OPs in the protein and isoenzyme patterns. As a result, the reactive species are reduced as the peroxidation processes are inhibited. Additionally, these native patterns may be normalized due to the enhanced functional groups associated with the phenolic compounds in the presence of Au-NPs. This is because they help the antioxidant system combat reactive intermediates that attack these biomacromolecules.[114] .

In terms of molecular assays, the liver tissues of the Etn-injected group showed a significant increase in the levels of relative expressions of the genes for caspase-3, p^{53}, and Bax, while Bcl2 gene expression decreased. This could be explained by the increased production of pro-apoptotic mediators after Etn injection[115] and the cell death induced by excessive ROS in the rats that received Etn injections.[116] The relative expression of apoptotic genes increased in the brain tissues of the Etn-injected group as Bcl2 protein expression decreased, particularly in the cerebrum and cerebellum. This could be explained by the generation of ROS, which releases stress signals and triggers the apoptotic machinery.[117–118] When rats received Etn injections, the administration of gold nano-extract controlled the production of mediators that promote and inhibit apoptosis. This was demonstrated by a decrease in the relative expression of p53, Bax, and Caspase-3 and an increase in the Bcl2 gene. Pro- and anti-apoptotic proteins are up- and down-regulated by the active phytoconstituents (flavonoids and polyphenolic compounds), which are well-known for their strong antioxidant, radical scavenging, and anti-inflammatory properties, according to **El Gamal *et al.***.[119] This finding is in line with their findings. Additionally, by directly interacting with superoxide anions and hydroxyl radicals, Au-NPs can form side products with reduced reactivity, which increases antioxidant activity [30,120].

5. Conclusion

Our results show that the hematological and biochemical alterations caused by Etn recovered to normal values upon administration of *C. equisetifolia* gold nano-extract. Fibrotic and inflammatory marker levels in the liver and brain tissues were found to have stabilized in the group that received nano-extract pretreatment. As a result, the pre-treated group had a greater reduction in the histopathological lesions caused by the Etn intoxication. Also, the gold nano-extract ameliorated the native electrophoretic patterns in the pre-treated group. The molecular analysis revealed that the relative expression of the apoptotic genes decreased significantly ($p \leq 0.05$) by the nano-extract compared to the rats that received Etn injections; however, their levels did not return to normal.

Authorship contributions.

The scientific notion was established by W.M.A., who also gathered pertinent prior studies. He designed the electrophoretic systems. The individuals who carried out biochemical experiments were N.E.I., A.K. H., and A.G.H. The investigations with molecules were carried out by W. K.B.K. and A.K.K. H.A. produced the plant extract and ethion solution that were given to the rats, and H.A.T. K.A.A. was in charge of the target tissues' histological analysis. Every author gave their approval to the manuscript's final draft. W.M.A. requested that the manuscript be published by contacting journal editors.

Ethics approval and consent to participate.

Under the number 131512012023, the Institutional Animal Ethics Committee of the National Research Center (Dokki, Giza, Egypt) authorized the experimental design for the animal groups.

Consent for publication

The authors consent to the publishing of identifiable details in the journal and paper, including the images included in the text.

CRediT authorship contribution statement

Wael Mahmoud Aboulthana: Writing – review & editing, Writing – original draft, Visualization, Project administration, Methodology, Formal analysis, Data curation, Conceptualization. **Noha El-Sayed Ibrahim:** Writing – original draft, Visualization, Methodology, Formal analysis, Data curation. **Amal Gouda Hussien:** Writing – original draft, Visualization, Methodology, Formal analysis, Data curation. **Amgad Kamal Hassan:** Writing – original draft, Visualization, Methodology, Data curation, Conceptualization. **Wagdy K.B. Khalil:** Writing – original draft, Methodology, Investigation, Formal analysis, Data curation. **Hassan Abdel-Gawad:** Writing – original draft, Visualization, Methodology, Formal analysis, Data curation, Conceptualization. **Hamdy Ahmed Taha:** Writing – original draft, Visualization, Methodology, Formal analysis, Data curation. **Ayda K. Kelany:** Data curation, Formal analysis, Methodology, Validation, Writing – original draft. **Kawkab A. Ahmed:** Writing – original draft, Visualization, Methodology, Formal analysis, Data curation, Conceptualization.

Declaration of competing interest

The authors declare that they have no known competing financial interests or personal relationships that could have appeared to influence the work reported in this paper.

Acknowledgements

The National Research Centre in Dokki, Giza, Egypt, provided the technological facilities needed for this study, for which the authors are grateful. They also appreciate the help of their colleagues in processing gold plant nano-extracts.

Appendix A. Supplementary data

Supplementary data to this article can be found online at https://doi.org/10.1016/j.jgeb.2025.100495.

References

1. Kuiper G, Young BN, WeMott S, et al. Factors associated with levels of organophosphate pesticides in household dust in agricultural communities. *Int J Environ Res Public Health*. 2022;19(2):862.
2. Selmi S, Rtibi K, Grami D, et al. Malathion, an organophosphate insecticide, provokes metabolic, histopathologic and molecular disorders in liver and kidney in prepubertal male mice. *Toxicol Rep*. 2018;5:189–195.
3. Tsai Y-H, Lein PJ. Mechanisms of organophosphate neurotoxicity. *Curr Opin Toxicol*. 2021;26:49–60.
4. Belin AC, Ran C, Anvret A, et al. Association of a protective paraoxonase 1 (PON1) polymorphism in Parkinson's disease. *Neurosci Lett*. 2012;522(1):30–35.
5. Kanthasamy A, Jin H, Charli A, et al. Environmental neurotoxicant-induced dopaminergic neurodegeneration: a potential link to impaired neuroinflammatory mechanisms. *Pharmacol Ther*. 2019;197:61–82.
6. dos Santos AA, Naime AA, de Oliveira J, et al. Long-term and low-dose malathion exposure causes cognitive impairment in adult mice: evidence of hippocampal mitochondrial dysfunction, astrogliosis and apoptotic events. *Arch Toxicol*. 2016;90(3):647–660.
7. Verma G, Chandra SM, Ramneek V, et al. Long-term exposures to ethion and endotoxin cause lung inflammation and induce genotoxicity in mice. *Cell Tissue Res*. 2019;375(2):493–505.
8. Badr AM. Organophosphate Toxicity: Updates of Malathion Potential Toxic Effects in Mammals and Potential Treatments. *Environ Sci Pollut Res*. 2020;27(21):26036–26057.
9. Lee KH, Cha M, Lee BH. Neuroprotective Effect of Antioxidants in the Brain. *Int J Mol Sci*. 2020;21(19):7152.
10. Abdel-Salam OM, Youness ER, Mohammed NA, et al. Nitric oxide synthase inhibitors protect against brain and liver damage caused by acute malathion intoxication. *Asian Pac J Trop Med*. 2017;10:773–786.
11. Akbel E, Arslan-Acaroz D, Demirel HH, et al. The subchronic exposure to malathion, an organophosphate pesticide, causes lipid peroxidation, oxidative stress, and tissue damage in rats: The protective role of resveratrol. *Toxicol Res*. 2018;7:503–512.
12. Linic S, Aslam U, Boerigter C, et al. Photochemical transformations on plasmonic metal nanoparticles. *Nat Mater*. 2015;14(6):567–576.
13. Liu R, Lal R. Potentials of engineered nanoparticles as fertilizers for increasing agronomic productions. *Sci Total Environ*. 2015;514:131–139.
14. Sun H, Jia J, Jiang C, et al. Nanoparticle-Induced Cell Death and Potential Applications in Nanomedicine. *Int J Mol Sci*. 2018;19:754.
15. Abdelhalim MA, Moussa SA. The gold nanoparticle size and exposure duration effect on the liver and kidney function of rats: *In vivo*. *Saudi J Biol Sci*. 2013;20(2):177–181.
16. Ilinskaya AN, Clogston JD, McNeil SE, et al. Induction of oxidative stress by Taxol® vehicle Cremophor-EL triggers production of interleukin-8 by peripheral blood mononuclear cells through the mechanism not requiring de novo synthesis of mRNA. *Nanomedicine*. 2015;11(8):1925–1938.
17. Chandrakala V, Aruna V, Angajala G. Review on metal nanoparticles as nanocarriers: current challenges and perspectives in drug delivery systems. *Emergent Mater*. 2022;5:1593–1615.
18. Gioria S, Vicente JL, Barboro P, et al. A combined proteomics and metabolomics approach to assess the effects of gold nanoparticles *in vitro*. *Nanotoxicology*. 2016;10(6):736–748.
19. Chueh PJ, Liang RY, Lee YH, et al. Differential cytotoxic effects of gold nanoparticles in different mammalian cell lines. *J Hazard Mater*. 2014;264:303–312.
20. Rizwan H, Mohanta J, Si S, et al. Gold nanoparticles reduce high glucose-induced oxidative-nitrosative stress regulated inflammation and apoptosis via tuberin-mTOR/NF-κB pathways in macrophages. *Int J Nanomedicine*. 2017;12:5841–5862.
21. Suh KS, Lee YS, Seo SH, et al. Gold nanoparticles attenuates antimycin A-induced mitochondrial dysfunction in MC3T3-E1 osteoblastic cells. *Biol Trace Elem Res*. 2013;153:428–436.
22. Han R, Xiao Y, Bai Q, et al. Self-therapeutic metal-based nanoparticles for treating inflammatory diseases. *Acta Pharm Sin B*. 2023;13(5):1847–1865.
23. Ying S, Guan Z, Ofoegbu PC, et al. Green synthesis of nanoparticles: Current developments and limitations. *Environ Technol Innov*. 2022;26, 102336.
24. Lu F, Sun D, Huang J, et al. Plant-mediated synthesis of Ag–Pd alloy nanoparticles and their application as catalyst toward selective hydrogenation. *ACS Sustainable Chem Eng*. 2014;2(5):1212–1218.
25. Zuhrotun A, Oktaviani DJ, Hasanah AN. Biosynthesis of Gold and Silver Nanoparticles Using Phytochemical Compounds. *Molecules*. 2023;28(7):3240.
26. Aher AN, Pal SC, Patil UK, et al. Evaluation of preliminary anticancer activity of *Casuarina equisetifolia* Frost (*Casuarinaceae*). *Planta Indica*. 2008;4:45–48.
27. Kantheti USK, Kumar DY, Ganinna B, et al. *Casuarina equisetifolia* effect as antidiabetic and antihyperlipidemic on streptozocin induced rats with diabetes. *IJCTPR*. 2014;2(3):432–436.
28. Zhang J, Weng Y, Ye D, et al. The complete chloroplast genome sequence of *Casuarina equisetifolia*. *Mitochondrial DNA B Resour*. 2021;6(10):3046–3048.
29. Aboulthana WM, Ibrahim NE, Hassan AK, et al. The hepato- and neuroprotective effect of gold *Casuarina equisetifolia* bark nano-extract against Chlorpyrifos-induced toxicity in rats. *J Genet Eng Biotechnol*. 2023;21:158.
30. Aboulthana WMK, Refaat E, Khaled SE, et al. Metabolite Profiling and Biological Activity Assessment of *Casuarina equisetifolia* Bark after Incorporating Gold Nanoparticles. *Asian Pac J Cancer Prev*. 2022;23(10):3457–3471.
31. Raj J, Chandra M, Dogra TD, et al. Determination of median lethal dose of combination of endosulfan and cypermethrin in wistar rat. *Toxicol Int*. 2013;20(1):1–5.
32. Al-Attar AM. Physiological effects of some plant oils supplementation on streptozotocin-induced diabetic rats. *Merit Res J Med Med Sci*. 2010;5:55–71.
33. Al-Attar AM, Al-Rethea HA. Chemoprotective effect of omega-3 fatty acids on thioacetamide induced hepatic fibrosis in male rats. *Saudi J Biol Sci*. 2017;24:956–965.
34. Gorun V, Proinov L, Baltescu V, et al. Modified Ellman Procedure for Assay of Cholinesterase in Crude Enzymatic Preparations. *Anal Biochem*. 1978;86(1):324–326.
35. Ellman GL, Courtney KD, Andres Jr V, et al. A New and Rapid Colorimetric Determination of Acetyl-cholinesterase Activity. *Biochem Pharmacol*. 1961;7(2):88–95.
36. Koracevic D, Koracevic G, Djordjevic V, et al. Method for the measurement of antioxidant activity in human fluids. *J Clin Pathol*. 2001;54(5):356–361.
37. Beutler E, Duron O, Kelly BM. Improved method for the determination of blood glutathione. *J Lab Clin Med*. 1963;61:882–890.
38. Sun Y, Oberley LW, Li Y. A Simple Method for Clinical Assay of Superoxide Dismutase. *Clin Chem*. 1988;34:479–500.
39. Aebi H. Catalase *in vitro*. *Methods Enzymol*. 1984;105:121–126.
40. Paglia DE, Valentine WN. Studies on the Quantitive and Qualitative Charecterization of Erythrocyte Glutathione Peroxidase. *J Lab Clin Med*. 1967;70(1):158–163.
41. Ohkawa H, Ohishi N, Yagi K. Assay for lipid peroxides in animal tissues by thiobarbituric acid reaction. *Anal Biochem*. 1979;95:351–358.
42. Levine RL, Williams JA, Stadtman ER, et al. Carbonyl assays for determination of oxidatively modified proteins. *Methods Enzymol*. 1994;233:346–357.
43. March CJ, Mosley B, Larsen A, et al. Cloning, sequence and expression of two distinct human interleukin-1 complementary DNAs. *Nature*. 1985;315:641–647.
44. Engelmann H, Novick D, Wallach D. Two tumor necrosis factor-binding proteins purified from human urine. Evidence for immunological cross-reactivity with cell surface tumor necrosis factor receptors. *J Biol Chem*. 1990;265:1531–1563.
45. Reddy GK, Enwemeka CS. A simplified method for the analysis of hydroxyproline in biological tissues. *Clin Biochem*. 1996;29:225–229.
46. El Mouedden M, Haseldonckx M, Mackie C, et al. Method for the determination of the levels of β-amyloid peptide in the CSF sampled from freely moving rats. *J Pharmacol Toxicol Methods*. 2005;52(2):229–233.
47. Suvarna SK, Layton C, Bancroft JD. *Bancroft's theory and practice of histological techniques*. Oxford: Churchill Livingstone Elsevier; 2019.
48. Fouad GI, Ahmed KA. Curcumin Ameliorates Doxorubicin-Induced Cardiotoxicity and Hepatotoxicity Via Suppressing Oxidative Stress and Modulating iNOS, NF-κB, and TNF-α in Rats. *Cardiovasc Toxicol*. 2022;22(2):152–166.
49. Bradford MM. A rapid and sensitive method for the quantitation of microgram quantities of protein utilizing the principle of protein-dye binding. *Anal Biochem*. 1976;72(1–2):248–254.
50. Darwesh OM, Moawad H, Barakat OS, et al. Bioremediation of textile reactive blue azo dye residues using nanobiotechnology approaches. *Res J Pharm, Biol Chem Sci*. 2015;6(1):1202–1211.
51. Subramaniam HN, Chaubal KA. Evaluation of intracellular lipids by standardized staining with a Sudan black B fraction. *J Biochem Bioph Methods*. 1990;21(1):9–16.
52. Abd Elhalim SA, Sharada HM, Abulyazid I, et al. Ameliorative effect of carob pods extract (*Ceratonia siliqua* L.) against cyclophosphamide induced alterations in bone marrow and spleen of rats. *J App Pharma Science*. 2017;7(10):168–181.
53. Siciliano MJ, Shaw CR. Separation and visualization of enzymes on gels. In 'Chromatographic and Electrophoretic Techniques. Vol. 2. Zone Electrophoresis'. 4th Edn.(Ed. I. Smith.), 1976; pp. 185-209.
54. Rescigno A, Sanjust E, Montanari L, et al. Detection of laccase, peroxidase, and polyphenol oxidase on a single polyacrylamide gel electrophoresis. *Anal Lett*. 1997;30(12):2211–2220.
55. Rammesmayer G, Praznik W. Fast and sensitive simultaneous staining method of Q-enzyme, α-amylase, R-enzyme, phosphorylase and soluble starch synthase separated by starch: polyacrylamide gel electrophoresis. *J Chromatogr*. 1992;623(2):399–402.

56. Ahmad A, Maheshwari V, Ahmad A, et al. Observation of esterase-like-albumin activity during N'-nitrosodimethyl amine induced hepatic fibrosis in a mammalian model. *Maced J Med Sci.* 2012;5(1):55–61.
57. Nei M, Li WS. Mathematical model for studing genetic variation in terms of restriction endonuclease. *Proc Natl Acad Sci USA*. 1979;76:5269–5273.
58. Wang J, Deng X, Zhang F, et al. ZnO nanoparticle-induced oxidative stress triggers apoptosis by activating JNK signaling pathway in cultured primary astrocytes. *Nanoscale Res Lett.* 2014;9(1):1–12.
59. Campana AD, Sanchez F, Gamboa C, et al. Dendritic morphology on neurons from prefrontal cortex, hippocampus, and nucleus accumbens is altered in adult male mice exposed to repeated low dose of malathion. *Synapses.* 2008;62:283–290.
60. Lasram MM, Lamine AJ, Dhouib IB, et al. Antioxidant and anti-inflammatory effects of N-acetylcysteine against malathion-induced liver damages and immunotoxicity in rats. *Life Sci.* 2014;107:50–58.
61. Chen H, Ng JPM, Tan Y, et al. Gold nanoparticles improve metabolic profile of mice fed a high-fat diet. *J Nanobiotechnol.* 2018;16(1):11.
62. Chekchaki N, Khaldi T, Rouibah Z, et al. Anti-Inflammatory and Antioxidant Effects of Two Extracts from *Pistacia lentiscus* in Liver and Erythrocytes, in an Experimental Model of Asthma. *International Journal of Pharmaceutical Sciences Review and Research.* 2017;42(1):77–84.
63. Li D, Huang Q, Lu M, et al. The organophosphate insecticide chlorpyrifos confers its genotoxic effects by inducing DNA damage and cell apoptosis. *Chemosphere.* 2015;135:387–393.
64. Mohammod Mostakim G, Zahangir M, Monir Mishu M, et al. Alteration of blood parameters and histoarchitecture of liver and kidney of silver barb after chronic exposure to quinalphos. *Journal of Toxicology.* 2015;2015, 415984.
65. Tamizhazhagan V, Pugazhendy K. The toxicity effect of monocrotophos 36% e. C on the haematology, Labeo rohita (Hamilton, 1882). International Journal of Current Pharmaceutical Research. 2015; 7(4): 92-95.
66. Abhijith BD, Ramesh M, Poopal RK. Sublethal toxicological evaluation of methyl parathion on some haematological and biochemical parameters in an Indian major carp Catla catla. *Comp Clin Pathol*. 2012;21(1):55–61.
67. Deabes MM, Aboulthana WM, Ahmed KA, et al. Assessment of the Ameliorative Effect of *Bacillus subtilis* against the Toxicity Induced by Aflatoxin B1 in Rats. *Egypt J Chem.* 2021;64(4):2141–2164.
68. Jothikrishnan SVTK, Gowrie SU. Phytochemical analysis and *in vitro* studies on antibacterial, antioxidant and anti-inflammatory activities using *Casuarina equisetifolia* bark extracts. *Int J Pharm Pharm Sci.* 2018;10(1):118–125.
69. Munir S, Liu ZW, Tariq T, et al. Delving into the Therapeutic Potential of *Carica papaya* Leaf against Thrombocytopenia. *Molecules.* 2022;27(9):2760.
70. Hernández AF, Gil F, Lacasaña M, et al. Modulation of the Endogenous Antioxidants Paraoxonase-1 and Urate by Pesticide Exposure and Genetic Variants of Xenobiotic-Metabolizing Enzymes. *Food Chem Toxicol.* 2013;61:164–170.
71. Esen M, Uysal M. Protective Effects of Intravenous Lipid Emulsion on Malathion-Induced Hepatotoxicity. *Bratisl Lek Listy.* 2018;119(6):373–378.
72. El-Shamarka MEA, Aboulthana WM, Omar NI, et al. Evaluation of the biological efficiency of *Terminalia chebula* fruit extract against neurochemical changes induced in brain of diabetic rats: an epigenetic study. *Inflammopharmacology*. 2024; 32:1439–1460.
73. Bekheit RA, Aboulthana WM, Serag WM. Bio- and Phyto-chemical Study on *Nannochloropsis oculata* algal Extract Incorporated with Gold Nanoparticles, *in Vitro* Study. *Frontiers in Scientific Research and Technology.* 2023;5(1):1–17.
74. Kunnaja P, Chansakaow S, Wittayapraparat A, et al. *In Vitro* Antioxidant Activity of *Litsea martabanica* Root Extract and Its Hepatoprotective Effect on Chlorpyrifos-Induced Toxicity in Rats. *Molecules.* 2021;26:1906.
75. Al-Shinnawy MS, Hassan AR, Ismail DA, et al. The potential protective and therapeutic effects of aloe vera juice on malathion induced hepatotoxicity in rabbits. *Egypt J Hosp Med.* 2014;55:146–158.
76. Flehi-Slim I, Chargui I, Boughattas S, et al. Malathion-induced hepatotoxicity in male Wistar rats: Biochemical and histopathological studies. *Environ Sci Pollut Res.* 2015;22:17828–17838.
77. Aksoy L, Alper Y. The effects of royal jelly on oxidative stress and toxicity in tissues induced by malathion, an organophosphate insecticide. *J Hell Vet Med Soc.* 2019; 70:1517–1524.
78. Kata FS. Short-time effects of malathion pesticide on functional and Histological changes of liver and kidney in female mice. *Pak J Biol Sci.* 2020;23:1103–1112.
79. Almalki DA. The potential protective effect of sesame oil and canola oil on rats exposed to malathion. *Curr Sci Int.* 2019;8:687–698.
80. Abdel-Salam OM, Sleem AA, Youness ER, et al. Novel protective effects of brilliant blue G in acute malathion toxicity. *React Oxyg Species.* 2018;6:414–427.
81. Severcan Ç, Ekremoglu M, Sen B, et al. Acute effects of different doses of malathion on the rat liver. *Clin Exp Hepatol.* 2019;5:237.
82. Selmi S, Rtibi K, Grami D, et al. Malathion, an organophosphate insecticide, provokes metabolic, histopathologic and molecular disorders in liver and kidney in prepubertal male mice. Toxicol Rep. 2018; 5: 189-195.
83. Fındıklı HA, Bilge Z, Aydın H, et al. The combination of acute pancreatitis and toxic hepatitis developing secondary to exposure to malathion: A case report. *Acta Gastro-Enterol Belg.* 2018;81:333–335.
84. Abdulkareem AO, Igunnu A, Ala AA, et al. Leaf extract of Morinda lucida improves pancreatic beta-cell function in alloxan-induced diabetic rats. *Egypt J Basic Appl Sci.* 2019;6(1):73–81.
85. Kim JY, Lee WS, Seo SJ, et al. Effects of gold nanoparticles on normal hepatocytes in radiation therapy. *Transl Cancer Res.* 2022;11(8):2572–2581.
86. Zhu S, Jiang X, Boudreau MD, et al. Orally Administered Gold Nanoparticles Protect against Colitis by Attenuating Toll-like Receptor 4- and Reactive Oxygen/Nitrogen Species-Mediated Inflammatory Responses but Could Induce Gut Dysbiosis in Mice. *J Nanobiotechnol.* 2018;16:86.
87. Muhammad HL, Garba R, Abdullah AS, et al. Hypoglycemic and hypolipidemic properties of *Casuarina equisetifolia* leaf extracts in alloxan induced diabetic rats. *Pharmacol Res Mod Chin Med.* 2022;2, 100034.
88. Saoudi M, Ncir M, Ben Ali M, et al. Chemical components, antioxidant potential and hepatoprotective effects of *Artemisia campestris* essential oil against deltamethrin-induced genotoxicity and oxidative damage in rats. *Gen Physiol Biophys.* 2017;36:331–342.
89. Aboulthana WM, Omar NI, El-Feky AM, et al. Phyto- and biochemical study on cape gooseberry (*Physalis peruviana* L.) extract incorporated with metal nanoparticles against hepatic injury induced in rats. *Nat Prod Res*. 2024;38(16): 1–14.
90. Rajput A, Sharma R, Bharti R. Pharmacological activities and toxicities of alkaloids on human health. *Mater Today: Proc.* 2022;48:1407–1415.
91. Aboulthana WM, Youssef AM, Seif MM, et al. Comparative Study between *Croton tiglium* Seeds and *Moringa oleifera* Leaves Extracts, after Incorporating Silver Nanoparticles, on Murine Brains. *Egypt J Chem.* 2021;64(4):1709–1731.
92. Shahmahmoodi Z, Jafarinejad S, Hormozi-Nezhad MR, et al. Protective Effects of Gold Nanoparticles Against Malathion-Induced Cytotoxicity in Caco-2 Cell. *Acta Med Iran.* 2020;58(11):553–561.
93. Karabag-Coban F, Bulduk I, Liman R, et al. Oleuropein alleviates malathion-induced oxidative stress and DNA damage in rats. *Toxicol Environ Chem.* 2016;98: 101–108.
94. Turk E, Kandemir FM, Yildirim S, et al. Protective effect of hesperidin on sodium Arsenite-induced nephrotoxicity and hepatotoxicity in rats. *Biol Trace Elem Res.* 2019;189(1):95–108.
95. Bakhshayesh A, Eslami Farsani R, Seyedebrahimi R, et al. Evaluation of the Negative Effects of Opium Tincture on Memory and Hippocampal Neurons in the Presence of Chicory Extract. *Adv Biomed Res.* 2023;12:23.
96. El-Feky AM, Aboulthana WM. Chemical Composition of Lipoidal and Flavonoidal Extracts from Egyptian Olive Leaves with *in Vitro* Biological Activities. *Egypt J Chem.* 2023;66(SI 13):1903–1913.
97. Dkhil MA, Bauomy AA, Diab MS, et al. Antioxidant and hepatoprotective role of gold nanoparticles against murine hepatic schistosomiasis. *Int J Nanomedicine.* 2015;10:7467–7475.
98. Cheng B, Zhang H, Hu J, et al. The Immunotoxicity and Neurobehavioral Toxicity of Zebrafish Induced by Famoxadone-Cymoxanil. *Chemosphere.* 2020;247, 125870.
99. Farag OM, Abd-Elsalam RM, Ogaly HA, et al. Metabolomic Profiling and Neuroprotective Effects of Purslane Seeds Extract Against Acrylamide Toxicity in Rat's Brain. *Neurochem Res.* 2021;46(4):819–842.
100. Alanazi AZ, Alqahtani F, Mothana RAA, et al. Protective role of Loranthus regularis against liver dysfunction, inflammation, and oxidative stress in Streptozotocin diabetic rat model. *Evid-Based Complement Altern Med.* 2020;2020:1–8.
101. De Araújo Júnior RF, de Araújo AA, Pessoa JB, et al. Anti-inflammatory, analgesic and anti-tumor properties of gold nanoparticles. *Pharmacol Rep.* 2017;69(1): 119–129.
102. Aboulthana WM, Ismael M, Farghaly HS. Assessment of mutagenicity induced by toxic factors affecting ovarian tissue in rats by electrophoresis and molecular dynamic modeling. *Int J Curr Pharm Rev Res.* 2016;7:347–359.
103. Borgia VJF, Thatheyus AJ, Murugesan AG. Impact of electroplating industry effluent on the electrophoretic protein pattern of serum in the freshwater fish *Cyprinus carpio*. *Indian J Biochem Biophys.* 2019;56:460–465.
104. Raj J, Joseph B. Impact of Acetamiprid Toxicity on Electrophoretic Patterns inLiver, Brain and Gill Tissues of the Fish *Oreochromis mossambicus*. *International Journal of Zoological Research.* 2017;13:120–124.
105. Kotb GAM, Gh FAA, Ramadan KS, et al. Protective role of garlic against malathion induced oxidative stress in male albino rats. *Indian J Anim Res.* 2016;50(3): 324–329.
106. Adams BM, Canniff NP, Guay KP, et al. The Role of Endoplasmic Reticulum Chaperones in Protein Folding and Quality Control. *Prog Mol Subcell Biol.* 2021;59: 27–50.
107. El-Sayed AB, Aboulthana WM, El-Feky AM, et al. Bio and Phyto-chemical Effect of *Amphora coffeaeformis* Extract against Hepatic Injury Induced by Paracetamol in Rats. *Mol Biol Rep.* 2018;45(6):2007–2023.
108. Aboulthana WM, Ibrahim NE, Osman NM, et al. Evaluation of the biological efficiency of silver nanoparticles biosynthesized using *Croton tiglium* L. seeds extract against azoxymethane induced colon cancer in rats. *Asian Pac J Cancer Prev.* 2020;21(5):1369–1389.
109. Al-Enazi MM. Combined Therapy of Rutin and Silymarin has More Protective Effects on Streptozotocin-Induced Oxidative Stress in Rats. *Journal of Applied Pharmaceutical Science.* 2014;4(01):021–028.
110. De Freitas RB, Augusti PR, De Andrade ER, et al. Black Grape Juice Protects Spleen from Lipid Oxidation Induced by Gamma Radiation in Rats. *Food Biochem.* 2014; 38:119–127.
111. Abulyazid I, Abd Elhalim SA, Sharada HM, et al. Hepatoprotective Effect of Carob Pods Extract (*Ceratonia siliqua* L.) against Cyclophosphamide Induced Alterations in Rats. *Int J Curr Pharm Rev Res.* 2017;8(2):149–162.
112. Seif MM, Ahmed-Farid OA, Aboulthana WM. Evaluation of the Protective Effect of *Acacia senegal* Extract against di-(2-ethylhexyl phthalate) Induced Hepato- and Neurotoxicity in Rats. *Annual Research & Review in Biology.* 2017;19:1–17.
113. Aboulthana WM, El-Feky AM, Ibrahim NE, et al. Evaluation of the Pancreatoprotective Effect of *Nannochloropsis oculata* Extract against Streptozotocin-Induced Diabetes in Rats. *Journal of Applied Pharmaceutical Science.* 2018;8(06):046–058.

114. Abdel-Halim AH, Fyiad AA, Aboulthana WM, et al. Assessment of the Anti-diabetic Effect of *Bauhinia variegata* Gold Nano-Extract against Streptozotocin Induced Diabetes Mellitus in Rats. *Journal of Applied Pharmaceutical Science.* 2020;10(05): 077–091.
115. Nur G, Caylak E, Kilicle PA, et al. Immunohistochemical distribution of Bcl-2 and p53 apoptotic markers in acetamiprid-induced nephrotoxicity. *Open Med (wars).* 2022;17(1):1788–1796.
116. Ghamry HI, Aboushouk AA, Soliman MM, et al. Ginseng® Alleviates Malathion-Induced Hepatorenal Injury through Modulation of the Biochemical, Antioxidant, Anti-Apoptotic, and Anti-Inflammatory Markers in Male Rats. *Life (basel).* 2022;12 (5):771.
117. Jiang W, Li S, Hu S, et al. Fucosylated chondroitin sulfate from sea cucumber inhibited islets of langerhans apoptosis *via* inactivation of the mitochondrial pathway in insulin resistant mice. *Food Sci Biotechnol.* 2015;24:1105–1113.
118. Abu Zeid EH, Hussein MMA, Ali H. Ascorbic acid protects male rat brain from oral potassium dichromate-induced oxdative DNA damage and apoptotic changes: the expression patterns of caspase-3, P53, Bax, and Bcl-2 genes. *Environ Sci Pollut Res Int.* 2018;25(13):13056–13066.
119. El Gamal AA, AlSaid MS, Raish M, et al. Beetroot (*Beta vulgaris* L.) extract ameliorates gentamicin-induced nephrotoxicity associated oxidative stress, inflammation, and apoptosis in rodent model. *Mediat Inflamm.* 2014;2014, 983952.
120. Zhou Y-T, He W, Wamer WG, et al. Enzyme-mimetic effects of gold@platinum nanorods on the antioxidant activity of ascorbic acid. *Nanoscale.* 2013;5: 1583–1591.